Coordination Chemistry Reviews
Elsevier Publishing Company, Amsterdam
Printed in The Netherlands

FAR INFRARED SPECTRA AND LATTICE VIBRATIONS OF INORGANIC COMPLEX SALTS

ICHIRO NAKAGAWA

Department of Chemistry, Faculty of Science, The University of Tokyo, Hongo, Tokyo (Japan 113)

(Received March 20th, 1969)

CONTENTS

A INTRODUCTION

During the last few years the far infrared spectra of various complex salts have been measured. Bands corresponding to lattice vibrations due to the interaction between complex ions and outer ions, as well as those of the metal–ligand vibrations in the complex ion, have been observed. An interpretation of the lattice vibrations yields important information regarding the interaction between the complex ions and the outer ions, in other words the interionic forces in the crystal.

The intramolecular (internal) vibration modes of the complex ion in the low frequency region are more or less coupled with the lattice (external) modes and accordingly the metal–ligand vibrations are correctly interpreted on the basis of the whole crystal model including the outer ions as well as the complex ion concerned.

In this review the far infrared spectra and lattice vibrations of some fundamental types of complex salts with the cubic, tetragonal and monoclinic structures will be discussed. Before discussing individual problems, a survey will be given of the lattice vibrations of ionic crystals observed by optical methods—optically active lattice vibrations—, since the interaction between the complex ions and outer ions may arise primarily from an ionic character.

B. OPTICALLY ACTIVE LATTICE VIBRATIONS OF CRYSTALS

(i) *Vibrations of a diatomic chain*

Consider a one-dimensional infinite chain composed of different types of atoms 1 and 2 occupying alternate positions (Fig. 1). This model includes various features common to lattice vibrations in general[1]. This chain forms a linear lattice with two atoms in the "Bravais primitive cell". Here the "Bravais primitive cell" is defined as the smallest unit in which no two groups of atoms become equivalent by a simple translation[2].

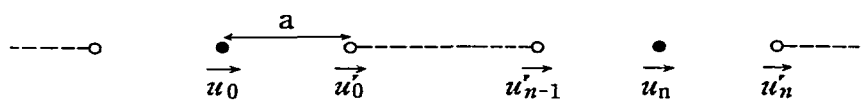

Fig. 1. One dimensional diatomic crystal.

If one restricts the atoms to move along the chain, the equations of motion for the two kinds of atoms can be described as:

$$m\ddot{u}_n = \beta[(u'_n - u_n) - (u_n - u'_{n-1})] \tag{1}$$

$$m'\ddot{u}'_n = \beta[(u_{n+1} - u'_n) - (u'_n - u_n)] \tag{2}$$

where u_n and u'_n denote the displacements of 1 and 2 atoms in the cell indexed by n, m and m' the masses of 1 and 2 atoms and β the potential constant for the bond between 1 and 2 atoms. The solutions for the above simultaneous equations (infinite in number) are as follows:

$$u_n = u \exp[i(\omega t + 2n\eta a)] \tag{3}$$

$$u'_n = u' \exp[i(\omega t + 2n\eta a)] \tag{4}$$

$$\omega^2 = \beta\left(\frac{1}{m} + \frac{1}{m'}\right) + \beta\left[\left(\frac{1}{m} + \frac{1}{m'}\right)^2 - \frac{4\sin^2 \eta a}{mm'}\right]^{\frac{1}{2}} \quad \text{(optical)} \tag{5}$$

$$\omega^2 = \beta\left(\frac{1}{m} + \frac{1}{m'}\right) - \beta\left[\left(\frac{1}{m} + \frac{1}{m'}\right)^2 - \frac{4\sin^2 \eta a}{mm'}\right]^{\frac{1}{2}} \quad \text{(acoustical)} \tag{6}$$

Here ω's are the angular frequencies ($\omega = 2\pi\nu$; ν = frequency) and η is the so-called wave vector and corresponds to the phase difference for each successive cell. For a given η which can take any value between $-\pi/2a$ and $\pi/2a$, there are two values for the frequency, and they constitute two branches, acoustical and optical

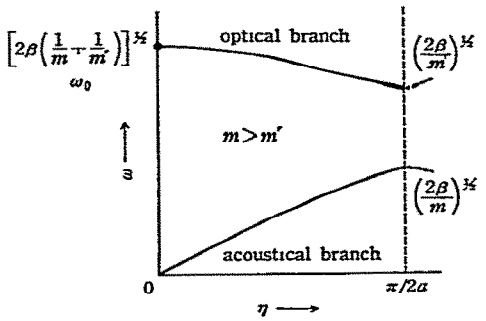

Fig 2 Relation between lattice frequencies of crystal (ω) and wave vector (η) for a one-dimensional diatomic crystal

branches, as shown in Fig. 2. The frequency at $\eta = 0$, the in-phase vibration frequency of the optical branch, can be observed by optical methods and is called "optically active lattice frequency". This frequency is calculated as:

$$\omega(\eta = 0) = \left[2\beta\left(\frac{1}{m} + \frac{1}{m'}\right)\right]^{\frac{1}{2}} \equiv \omega_0 \quad \text{(optical)} \tag{7}$$

while for the acoustical branch:

$$\omega(\eta = 0) = 0 \quad \text{(acoustical)} \tag{8}$$

The corresponding amplitude ratio is given by:

$$u/u' = -m'/m \quad \text{or} \quad mu + m'u' = 0 \quad \text{(optical)} \tag{9}$$

and

$$u = u' \quad \text{(acoustical)} \tag{10}$$

This means that, for the optical vibration, the center of mass of each cell remains stationary while in the acoustical vibration the two atoms move as one unit, corresponding to translational motion of the crystal as a whole.

For the two-dimensional and three-dimensional lattices as shown in Fig. 3,

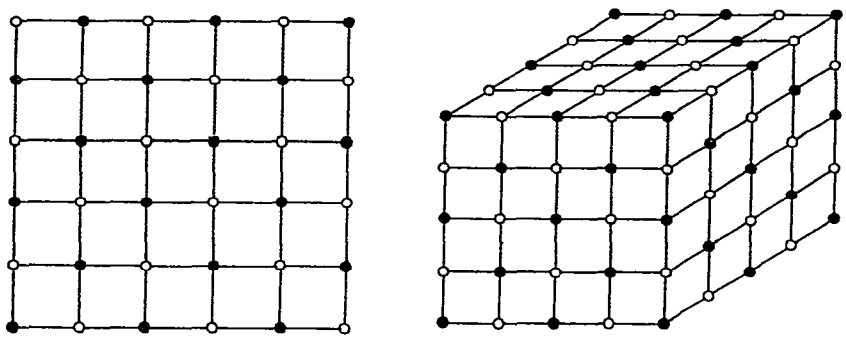

Fig 3 Two-dimensional (a) and three-dimensional (b) diatomic crystals.

the doubly degenerate and triply degenerate infrared-active vibration frequencies are also given by Eq. (7), if only the stretching potential constant between the nearest atom pairs is taken into consideration. The vibration frequency in wave-numbers is written as:

$$\tilde{\nu}(\mathrm{cm}^{-1}) = \frac{1}{2\pi c}\sqrt{2\beta\left(\frac{1}{m}+\frac{1}{m'}\right)} \tag{11}$$

It is to be noted that the vibrational frequency for the diatomic free molecule is

$$\tilde{\nu}(\mathrm{cm}^{-1}) = \frac{1}{2\pi c}\sqrt{\beta\left(\frac{1}{m}+\frac{1}{m'}\right)} \tag{11'}$$

The frequency for a diatomic crystal is different from this by a factor of 2β instead of β in the potential constant part.

(ii) GF-matrix method for calculation of optically active lattice frequencies

Wilson's GF-matrix method[3] may also be applied to the calculation of optically active lattice frequencies of crystals and has been described in detail in a paper by Shimanouchi, Tsuboi and Miyazawa[4]. An outline of this method is described below.

The first procedure of the normal coordinate analysis is to describe the free molecule by using Cartesian displacement coordinates:

$$T = \tfrac{1}{2}\sum_i m_i(\dot{x}_i^2+\dot{y}_i^2+\dot{z}_i^2) = \tfrac{1}{2}\tilde{\dot{\boldsymbol{X}}}\boldsymbol{M}\dot{\boldsymbol{X}} \tag{12}$$

$$\begin{aligned} V &= \tfrac{1}{2}K_1(\Delta r_1)^2+\tfrac{1}{2}K_2(\Delta r_2)^2+\ldots+k_1(\Delta r_1)(\Delta r_2)+\ldots \\ &= \tfrac{1}{2}f_{11}R_1^2+\tfrac{1}{2}f_{22}R_2^2+\ldots+f_{12}R_1R_2+\ldots \\ &= \tfrac{1}{2}\tilde{\boldsymbol{R}}\boldsymbol{F}\boldsymbol{R} \end{aligned} \tag{13}$$

$$\boldsymbol{R} = \boldsymbol{B}\boldsymbol{X} \tag{14}$$

$$V = \tfrac{1}{2}\tilde{X}\tilde{B}FBX = \tfrac{1}{2}\tilde{X}F_xX \tag{15}$$

$$F_x = \tilde{B}FB \tag{16}$$

$$| M^{-1}F_x - E\lambda | = 0 \tag{17}$$

$$\nu_i(\mathrm{cm}^{-1}) = (1/2\pi c)\sqrt{\lambda_i} \tag{18}$$

$$X = L_xQ \tag{19}$$

$$M^{-1}F_xL_x = L_x\Lambda \tag{20}$$

Here

X: column matrix corresponding to the Cartesian displacement coordinates such as Δx_1, Δy_1, Δz_1, ...

R: column matrix corresponding to the internal coordinates such as Δr_1, $\Delta\phi_1$, Δq_1, ...

F: potential energy matrix

B: transformation matrix between R and X

F_x: potential energy matrix in terms of Cartesian displacement coordinates

L_x: transformation matrix between the Cartesian displacement coordinates and the normal coordinates Q, which supplies the displacement of each atom for each vibration.

In the normal coordinate treatment of optically active vibrations of a crystal, the optically active Cartesian displacement coordinates X_{op} and internal coordinates R_{op} are set up as:

$$X_{op} = N_x \sum_{ijk} X_{ijk} \tag{21}$$

$$R_{op} = N_R \sum_{ijk} R_{ijk} \tag{22}$$

where X_{ijk} and R_{ijk} are respectively the Cartesian displacement and internal coordinates associated with the three-dimensional Bravais primitive cell (ijk). These are summed up for all the cells so that X_{op} and R_{op} which describe the in-phase motions of all the cells corresponding to $\eta = 0$ may be obtained (see Eqs (3, 4)). The optically active B matrix, B_{op} is defined as:

$$R_{op} = B_{op}X_{op} \tag{23}$$

and is calculated as:

$$B_{op} = \sum_{i'j'k'} B_{ijk,i'j'k'} \tag{24}$$

where $B_{ijk,i'j'k'}$ is the submatrix associated with the internal coordinates R_{ijk} of the cell ijk and the Cartesian displacement coordinates $X_{i'j'k'}$ of the cell $i'j'k'$. The F matrix in terms of internal coordinates for the optically active vibrations is given by:

$$F_{op} = \sum_{ijk} F_{ijk,i'j'k'} \tag{25}$$

where $F_{ijk,i'j'k'}$ is the submatrix corresponding to the cells ijk and $i'j'k'$. ($F_{ijk,ijk}$ denotes the diagonal submatrix with respect to each Bravais primitive cell).

In a similar manner, as for free molecule calculation described above, the vibrational frequencies are calculated as follows:

$$V_{op} = \tfrac{1}{2}\tilde{X}_{op}F_{op}X_{op} \tag{26}$$

$$F_{xop} = \tilde{B}_{op}F_{op}B_{op} \tag{27}$$

$$(M^{-1}F_{xop})L_x = L_x\Lambda \tag{28}$$

From the eigenvalues and eigenvectors of $(M^{-1}F_{xop})$ matrix, one can obtain the vibrational frequencies and vibrational modes of the optically active vibrations

The GF-matrix method may also be applied to the problem of a one-dimensional infinite chain discussed in the previous section (B, *i*) The B matrix is written as:

$$\begin{array}{c} \\ \vdots \\ \Delta r_{i-1} \\ \Delta r'_{i-1} \\ \Delta r_i \\ \Delta r'_i \\ \Delta r_{i+1} \\ \Delta r'_{i+1} \\ \vdots \end{array}
\begin{array}{c}
\cdots \Delta x_{i-1}^{(1)} \quad \Delta x_{i-1}^{(2)} \quad \Delta x_i^{(1)} \quad \Delta x_i^{(2)} \quad \Delta x_{i+1}^{(1)} \quad \Delta x_{i+1}^{(2)} \cdots \\
\left[\begin{array}{cccccc}
\ddots & & & & & \\
-1 & 1 & 0 & 0 & 0 & 0 \\
0 & -1 & 1 & 0 & 0 & 0 \\
0 & 0 & -1 & 1 & 0 & 0 \\
0 & 0 & 0 & -1 & 1 & 0 \\
0 & 0 & 0 & 0 & -1 & 1 \\
0 & 0 & 0 & 0 & 0 & -1 \\
 & & & & & \ddots
\end{array}\right]
\end{array} \tag{29}$$

By the use of Eq. (24), the B_{op} is calculated as:

$$B_{op} = \begin{bmatrix} 0 & 0 \\ 0 & 0 \end{bmatrix} + \begin{bmatrix} -1 & 1 \\ 0 & -1 \end{bmatrix} + \begin{bmatrix} 0 & 0 \\ 1 & 0 \end{bmatrix} = \begin{bmatrix} -1 & 1 \\ 1 & -1 \end{bmatrix} \tag{30}$$

If the potential energy V of this system is expressed as:

$$\begin{aligned} V = \tfrac{1}{2}K[\ . \ +(\Delta r_i)^2+(\Delta r'_i)^2+\ .\ ]+k[\ldots+(\Delta r_i)(\Delta r'_i)+\ldots] \\ +k'[\ldots+(\Delta r_i)(\Delta r'_{i-1})+\ldots] \end{aligned} \tag{31}$$

the F matrix becomes

$$
\begin{array}{c}
\\
\vdots \\
\Delta r_{i-1} \\
\Delta r'_{i-1} \\
\Delta r_i \\
\Delta r'_i \\
\Delta r_{i+1} \\
\Delta r'_{i+1} \\
\vdots
\end{array}
\begin{array}{c}
\begin{array}{cccccc}
\cdots \Delta r_{i-1} & \Delta r'_{i-1} & \Delta r_i & \Delta r'_i & \Delta r_{i+1} & \Delta r'_{i+1} \cdots
\end{array} \\
\left[\begin{array}{cccccc}
\ddots & & & & & \\
K & k & 0 & 0 & 0 & 0 \\
k & K & k' & 0 & 0 & 0 \\
0 & k' & K & k & 0 & 0 \\
0 & 0 & k & K & k' & 0 \\
0 & 0 & 0 & k' & K & k \\
0 & 0 & 0 & 0 & k & K \\
 & & & & & \ddots
\end{array}\right]
\end{array}
\tag{32}
$$

and by Eq. (25) the F_{op} is given as:

$$
F_{op} = \begin{bmatrix} 0 & k' \\ 0 & 0 \end{bmatrix} + \begin{bmatrix} K & k \\ k & K \end{bmatrix} + \begin{bmatrix} 0 & 0 \\ k' & 0 \end{bmatrix} = \begin{bmatrix} K & k+k' \\ k+k' & K \end{bmatrix} \tag{33}
$$

By solving the secular equation (28), one obtains

$$
\lambda_1 = 2\left(\frac{1}{m} + \frac{1}{m'}\right)(K-k-k') \tag{34}
$$

$$
\lambda_2 = 0 \tag{35}
$$

where λ_1 and λ_2 correspond to the optical and acoustical vibrational frequencies at $\eta = 0$ (see Eqs. (7, 8) in section (B, 1)).

(*iii*) *Interionic potential constants of diatomic ionic crystals*

The interionic force in the diatomic crystal like NaCl, which may be regarded

TABLE 1

LATTICE FREQUENCIES (ν), INTERIONIC POTENTIAL CONSTANTS (β) AND INTERIONIC DISTANCES (r) OF SOME ALKALI HALIDES*

Compound	ν (cm^{-1})**	β(md/Å)	r(Å)
NaCl	165	$0\,11_2$	2 82
NaBr	140	$0\,10_3$	2 98
KCl	145	$0\,11_5$	3 15
KBr	122	$0\,11_5$	3 30
KI	103	$0\,09_3$	3 53
CsCl	102	$0\,08_6$	3 57
CsBr	82	$0\,09_9$	3 71
CsI	66	$0\,08_3$	3 95

* The crystal structures of Na- and K-salts are NaCl type (O_h^5, F m3m). Those of Cs salts are CsCl type (O_h^1, P m3m). The lattice frequency of the CsCl type crystal is also given by eq. (11).
** The observed frequencies are taken from the review by Miller[5].

as the first derivative of the potential energy with respect to interionic distance ($-\delta V/\delta r$), consists of various terms. These terms may be divided into two parts, repulsive and attractive forces. In the equilibrium position these two terms are equal in magnitude. In the second derivative of the potential ($\delta^2 V/\delta r^2$), the repulsion term may be much larger than the attraction term resulting in a positive value of the potential constant (force constant). If one neglects the long-range force and takes into consideration only the interaction between the nearest ion pairs, $(\delta^2 V/\delta r^2)_{\text{repulsive}}$ may primarily govern the lattice frequencies. Therefore one of the approaches to analyze the lattice frequencies of ionic crystal is based on the molecular dynamical model in which the optical frequency ω_0 at $\eta = 0$ is evaluated by the local elastic restoring force (the force constant β between the nearest ion pairs). Table 1 gives the lattice frequencies and corresponding potential constants calculated from Eq. (11) for alkali halide ionic crystals[5]. It can be seen that the value of potential constants corresponding to typical ionic bonds is about 0.1 mdyn/Å, which is much smaller than those obtained for covalent bonds such as in Cl_2 (3.2 mdyn/Å).

(*iv*) *Factor group analysis for optically active vibrations of complex salts*

If the Bravais primitive cell contains p atoms, there are $3p$-3 optical vibrations and 3 acoustical vibrations. The $3p$-3 optical vibrations of the complex salts may be classified as internal (intramolecular) vibrations in the complex ion and external (lattice) vibrations, although the internal and external vibrations are more or less coupled with each other. Based on the knowledge of the space group of the crystal, the $3p$-3 optical and 3 acoustical vibrations are classified into each symmetry species, using a method analogous to the normal vibrations of free molecules. This analysis for the crystal vibrations may be called "factor group analysis", and is described below, using as an example $K_3[Fe(CN)_6]$, for which the far infrared spectra and lattice vibrations will be discussed later.

The number of vibrations (n_i) of each symmetry species (i), that is, in each irreducible representation is given by

$$n_i = (1/g) \sum_{\rho} g_\rho \chi_i(R) \chi'_\rho(R) \tag{36}$$

where χ_i (R) and χ'_ρ (R) are the characters of the operation R in the representation Γ_i and Γ, respectively, g is the order of the group and g_ρ is the number of the operations in the class ρ g, g_ρ and χ_i (R) can be taken from the character table for the space group. χ_ρ'(R) may be determined when the characters of the transformations of the displacement coordinates are known.

The crystal structure of $K_3[Fe(CN)_6]$ is monoclinic with the space group C_{2h}^5 ($P\ 2_1/c$; z = 2) and as shown in Fig. 4 the Bravais primitive cell contains 32 atoms, two kinds of $[Fe(CN)_6]^{3-}$ ions and six K^+ ions[6]. This crystal has

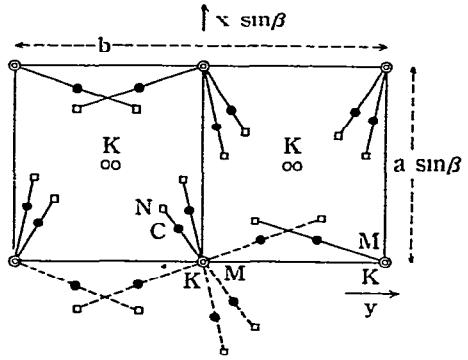

○M (Fe)	Fe(1)	0	0	0	
○ K	Fe(2)	0	b/2	c/2	
• C	K (1)	0	0	c/2	
▫ N	K (2)	0	b/2	0	
	K (3)	~a/2±b/4±c/4			
	K (4)				
	K (5)				
	K (6)				

Fig 4 Structure of $K_3[Fe(CN)_6]$ with the space group C_{2h}^5 ($P\,2_1/c$, z = 2)

screw axes 2_1 parallel to b axis and passing through (x = 0, z = ±1/4c) and (x = ±½a, z = ±1/4c), glide planes c perpendicular to b axis at (y = ±1/4b) and centers of symmetry 1 at (x = 0, y = 0, z = 0), (x = 0, y = 0, z = ±½c), etc. (see Fig. 4 and Table 2)

First, consider all degrees of freedom, then

$$[\chi'_\rho(R)]_N = U_R(p)\,[\pm 1 + 2\cos\phi_R] \tag{37}$$

and $n_i(N)$ obtained by substituting this $[\chi'_\rho(R)]_N$ into Eq. (36) includes all types of normal modes (translations, external and internal modes). $U_R(p)$ is the number of atoms which remains invariant under the operation R. According as R is a pure rotation (proper operation) through ϕ_R or a rotation through ϕ_R accompanied by a reflection (improper operation), a + or − sign is used (see Table 2 of the example $K_3[Fe(CN)_6]$).

Next, consider the acoustical modes. In this case $U_R(p)$ is to be put equal to 1 for all R, since the whole group moves as one unit. Therefore

$$[\chi'_\rho(R)]_T = \pm 1 + 2\cos\phi_R \tag{38}$$

and $n_i(T)$ is obtained in a similar way.

External (lattice) modes are further subdivided into translational and rotational lattice modes. Here one should account for the number of ions in the Bravais primitive cell. $U_R(s)$ represents the number of ions whose center of

TABLE 2

FACTOR GROUP ANALYSIS FOR OPTICALLY ACTIVE VIBRATIONS OF $K_3[Fe(CN)_6]$ CRYSTAL (C_{2h}^5, $P\,2_1/c$, $z = 2$)

C_{2h}^5	E	$g = 4$ 2_1	c	i	$n_i(N)$	$n_i(T)$	$n_i(T')$	$n_i(R')$	$n_i(n)$
A_g	1	1	1	1	21	0	3	3	15
A_u	1	1	−1	−1	27	1	8	0	18
B_g	1	−1	−1	1	21	0	3	3	15
B_u	1	−1	1	−1	27	2	7	0	18
$U_R(p)$	32	0	0	4	↑	↑	↑	↑	
$U_R(s)$	8	0	0	4					
$U_R(s-v)$	2	0	0	2					
$\pm 1+2\cos\Phi_R$	3	−1	1	−3					
$1\pm 2\cos\Phi_R$	3	−1	−1	3					
$[\chi_\rho'(R)]_N$	96	0	0	−12	←				
$[\chi_\rho'(R)]_T$	3	−1	1	−3	←	←			
$[\chi_\rho'(R)]_{T'}$	21	1	−1	−9	←		←		
$[\chi_\rho'(R)]_{R'}$	6	0	0	6	←			←	

$U_R(p)$: the number of atoms which remain invariant under operation R.
$U_R(s)$: the number of ions whose center of symmetry remains invariant under operation R
$U_R(s-v)$: the number of ions which are constitued by more than one atom among $U_R(s)$ ions
$n_i(N)$: the number of total freedom
$n_i(T)$ the number of translational motions of a crystal as a whole
$n_i(T')$ the number of translational lattice modes.
$n_i(R')$: the number of rotational lattice modes
$n_i(n)$: the number of internal modes in the complex ion

symmetry remains invariant under the operation R. Among these $U_R(s)$, the number of ions which are constituted by more than one atom, is designated by $U_R(s-v)$. Then the characters corresponding to the translational lattice modes $[\chi_\rho'(R)_T]$, and those for the rotational lattice modes $[\chi_\rho'(R)]_{R'}$, are given as:

$$[\chi_\rho'(R)]_{T'} = [U_R(s-1)]\,(\pm 1+2\cos\phi_R) \tag{39}$$

$$[\chi_\rho'(R)]_{R'} = U_R(s-v)\,(1 \pm 2\cos\phi_R) \tag{40}$$

From these characters, the numbers of the translational modes $n_i(T')$ and rotational lattice modes $n_i(R')$ are calculated.

Finally, the number of the internal modes (intramolecular modes in the complex ion) $n_i(n)$ may be obtained by direct subtraction of $n_i(T)$, $n_i(T')$, $n_i(R')$ from the total number of degree of freedom $n_i(N)$:

$$n_i(n) = n_i(N) - n_i(T) - n_i(T') - n_i(R')$$

These procedures mentioned above are summarized in Table 2 for the example of $K_3[Fe(CN)_6]$ with the space group C_{2h}^5 ($P2_1/c$).

C. EXPERIMENTAL METHODS

(i) *Spectrometer and device for low-temperature measurement*

For spectroscopic measurements in the far infrared region, both the diffraction and interferometric methods are available. As far as measurement down to 30 cm^{-1} is concerned, a spectrometer with a diffraction grating is more convenient to use for a chemical study than the interferometer. A vacuum and double-beam infrared spectrometer is most useful, if it is used carefully, especially in low-temperature measurement.

The results given in the present review were obtained using mainly the vacuum and double-beam HITACHI FIS-1 and FIS-3 far infrared spectrophotometers. For measurements at low temperature, down to liquid nitrogen temperature, a Dewar vessel (low temperature cell) is placed in the sample box which is kept at high vacuum ($10^{-4} \sim 10^{-5}$ mmHg). Samples are inserted into silicon plates contacted with the metal conductor or directly contacted with the conductor in the low temperature cell[7].

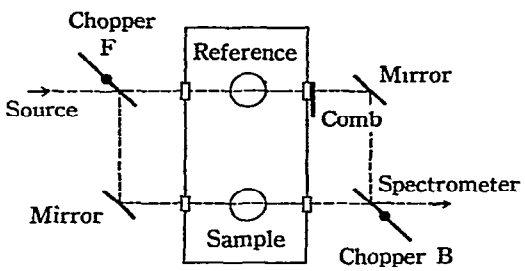

Fig 5 Chopper system of vacuum and double-beam Hitachi FIS-1 and -3 spectrophotometers in the far-infrared.

In the spectrometers are installed two choppers, F and B; one (F) is in front of a sample box, and the other (B) is behind a sample box as shown in Fig 5. For room temperature measurement a synchronous rotation is obtained for the two choppers. However, for low-temperature measurements the rotation of the chopper B should be stopped, in order to eliminate the temperature effect due to the temperature difference between the sample and reference sides, and the comb attenuator. By operating only the chopper F, about 50% of the sample beam and about 50% of the reference beam enter the spectrometer alternately. By fixing the chopper B at the appropriate position, one can adjust the 100% line of the spectrum.

In a FIS-3 spectrometer, a means for double-chopping is utilized. In addition to the choppers B and F of 10 cycles, another chopper is installed just behind the light source and is operated at 0 9 cycles in the case of the low-temperature

measurement, so that the temperature effect is eliminated without stopping the chopper B.

(ii) Determination of lattice frequencies

It has been shown that in the one-dimensional diatomic chain discussed in the previous section (B, i), atoms of one type move as one body against atoms of other type for the optical vibration $\omega_0(2\pi\nu_0)$ at $\eta = 0$. The procedure for determining this ν_0 frequency experimentally is described below.

This frequency ν_0 is the infrared dispersion frequency, or the resonant frequency, at which the refractive index and the dielectric constant become infinitely large. It would be measured as the absorption frequency (the frequency of the minimum transmission) of a thin film of a crystal, if such a thin specimen of a crystal would be prepared. However, in practice one can not prepare a thin film of a crystal to transmit sufficient radiation and so a direct determination of the ν_0 as a thickness $d \to 0$ is not possible. Therefore transmission measurements for the sample should be made in some other dispersing medium. In most of the examples discussed in the later sections of this review, transmission measurements were made for samples as finely divided powders dispersed in polyethylene and in a Nujol mull and the absorption frequencies for these samples were regarded as the ν_0's.

The reflection spectrum of a single crystal can also determine the ν_0's[8]. By transforming the reflectance data using the Kramers–Kronig relation, the real and imaginary parts of the complex dielectric constant ($\varepsilon' = n^2 - k^2$, $\varepsilon'' = 2nk$), where n is the refractive index and k is the absorption coefficient, are obtained. The maxima of the imaginary part ε'' supply the resonant frequencies. Making the assumption that the dispersion can be interpreted in terms of simple independent oscillator, the oscillator parameters (ν_0^i, $4\pi\rho_i$ and $\gamma_i\nu_0^i$; the resonant frequency, the strength and the line width of the i-th oscillator, respectively), are obtained by using the ε' and ε'' data. The difference between the resonant frequencies obtained from the reflection data of a crystal and those from the transmission data of a powder sample in other media is less than 5% for the lattice vibrations of an ionic crystal such as $KNiF_3$ and $KMgF_3$, according to the results by Perry *et al.*[9].

D. INDIVIDUAL COMPLEX SALTS

The discussion will mainly consider the results of several types of crystals studied by the author or his colleagues

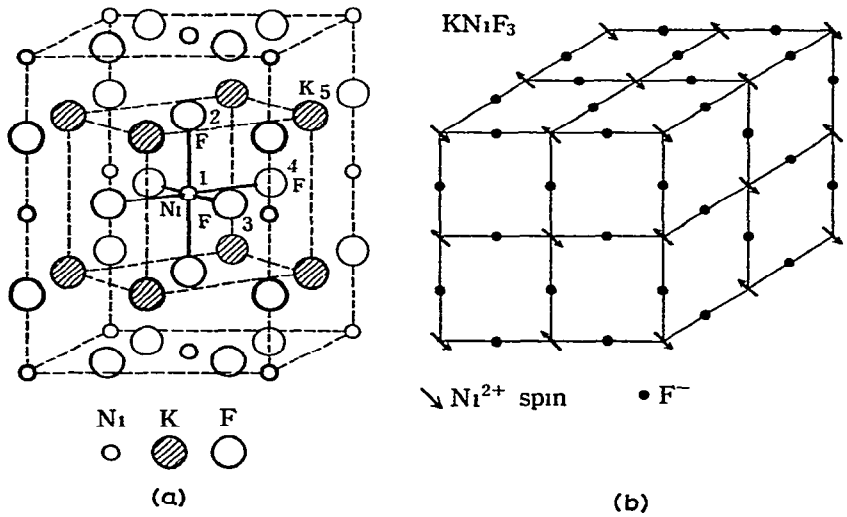

Fig. 6 Structure of $KNiF_3$ (a) arrangement of atoms; (b) magnetic structure.

(i) *Perovskite fluorides and rutile fluorides*

The far infra-red spectra and lattice vibrations of the so-called ionic crystal perovskite fluorides and their rutile counterparts are presented before discussion of the inorganic complex salts. Several investigations (Perry *et al.*[9], Balkanski *et al.*[10] and Barker[11]) have been made on the lattice vibrations and the nature of the interatomic forces in the crystal.

The crystal structure of $KNiF_3$ as well as $KMgF_3$ and $KZnF_3$ is of the regular cubic perovskite type with the space group O_h^1 as shown[12] in Fig. 6(a). $KNiF_3$ exhibits antiferromagnetism below[13] the Néel temperature 275° K and Fig. 6(b) shows the magnetic structure; the spin arrangement is due to the Ni^{2+} ions. This magnetic behaviour suggests a superexchange interaction of Ni^{2+} spins through F^- ions, in other words electron delocalization in the Ni–F bond. A study of how the magnetic behaviour of this ionic crystal is reflected in the lattice vibrations or interionic potential constants will be discussed below. The Bravais primitive cell for KMF_3 consists of five atoms, K, M and three F's (Fig 6(a)). Optically active lattice vibrations are $3f_{1u}+1f_{2u}$, of which the f_{2u} mode is inactive in the infra-red. There is also another f_{1u} acoustical vibration corresponding to the translational motion of a crystal as a whole.

The infra-red spectra of KMF_3 together with that of $NaNiF_3$ are given[14] in Fig. 7. The three absorption bands are observed for KMF_3 as expected for the cubic perovskite structure of O_h^1. Of these three bands the highest shifts by 10–20 cm^{-1} to higher frequency at low temperature, while the other two do not change their frequencies appreciably. These results are explained as follows. The highest band is assigned to the M–F stretching mode, in which the F^- ions

displace along the M–F–M line, while the second one is assigned to the M–F bending mode, in which the F^- ions displace perpendicularly to the M–F–M line (see ν_1 and ν_2 of Fig. 8 below). The lowest band is assigned to the K^+ ion lattice mode, in which the lattice of the K^+ ions displaces relative to the main lattice consisting of the M^{2+} and F^- ions (see ν_3 of Fig. 8). At low temperature the M–F bond becomes shorter, the M–F stretching force constant becomes larger, and, accordingly, the corresponding frequency becomes higher. The M–F bending force constant may not change as much as the stretching force constant and the bending frequency remains rather constant with temperature change. At low temperature both of the lattices consisting of the K^+ ions and of the M^{2+} and

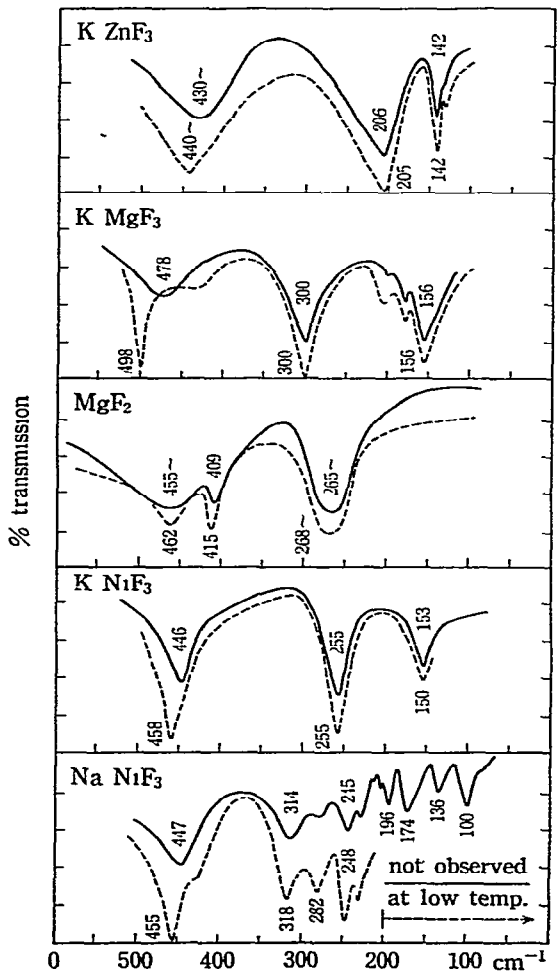

Fig. 7. Infrared absorption spectra of the perovskite fluorides and rutile fluoride MgF_2. Powdered samples dispersed in polyethylene (1–2 mg/cm²) and in the Nujol mull. ——, room temperature; – – – –, liquid-nitrogen temperature.

F^- ions contract and the interaction between these two lattices, which primarily governs the frequency of the lowest band, may not change much and accordingly may result in a small temperature effect on the lowest frequency. From the foregoing argument, the temperature effect yields experimental evidence for the above assignments of the three lattice modes. Other evidence for the assignments is given by comparison of the spectrum of $KMgF_3$ with that of MgF_2 as shown in Fig. 7, since no band is observed in the MgF_2 spectrum corresponding to the lowest one around 150 cm^{-1} in $KMgF_3$ which arises from the K^+ ion-lattice vibration. Further confirmation for the vibrational assignment of KMF_3 will be given later in the analysis of MF_2.

A more complicated spectrum is obtained with $NaNiF_3$ than KMF_3 as shown in Fig. 7. According to the X-ray analysis of this salt, the Ni–F–Ni bond is not linear but is bent[15]. The $NaNiF_3$ does not form a regular perovskite but shows a distorted structure giving rise to a complicated spectrum. The distorted structure of $NaNiF_3$ may be understood from the smaller ionic radius of the Na^+ ion. If the condition:

$$\text{(the sum of the ionic radii of } M^+ \text{ and } F^-) = \\ = \sqrt{2t}\,\text{(the sum of the ionic radii of } M^{2+} \text{ and } F^-) \tag{41}$$

$$0.89 < t < 1.00 \tag{42}$$

is satisfied for the $M'MF_3$ salt, it may form a regular perovskite[16]. As shown in Table 3, for $KNiF_3$, $KMgF_3$ and $KZnF_3$, this condition is satisfied. However,

TABLE 3

IONIC RADII AND FORMATION OF REGULAR CUBIC PEROVSKITE STRUCTURES

$M'MF_3$	$r(M'^+)$	$r(M^{2+})$	$r(F^-)$	t	*Comment*
$KNiF_3$	1 33 Å	0 70 Å	1 36 Å	0 92	OK
$KMgF_3$	1 33	0 65	1.36	0.95	OK
$KZnF_3$	1.33	0.74	1 36	0 91	OK
$NaNiF_3$	0 95	0 70	1 36	0 79	NO

for $NaNiF_3$, t amounts to 0.79, and this results in an appreciable distortion from the regular pervoskite structure. Again for $NaNiF_3$ the highest band due to the Ni–F stretching mode shifts to higher frequency by 8 cm^{-1} at low temperature.

The optically active lattice vibration frequencies are calculated according to the procedure outlined in the previous section (B,ii). The following type of potential function is used:

$$V = \tfrac{1}{2}\sum_i K(\Delta r_{MF}{}^i)^2 + \tfrac{1}{2}\sum_i H(r_{MF}\Delta\alpha_{FMF}{}^i)^2 + \tfrac{1}{2}\sum_i F(\Delta q_{F\ F}{}^i)^2 \\ + \tfrac{1}{2}\sum_i f_1(\Delta q'_{K.\ F}{}^i)^2 + \tfrac{1}{2}\sum_i f_2(\Delta q^*_{K\ M}{}^i)^2, \tag{43}$$

where K and H denote the M–F bond stretching and the F–M–F angle bending

force constants, respectively, F denotes the repulsion constant between the nearest nonbonded F^- ions, and f_1 and f_2 denote the interaction between K^+ and F^- and that between K^+ and M^{2+}, respectively. The valence force type potential was assumed for the MF_6-octahedron, taking into account the covalent character of the M–F bond, and the central force type potential was assumed for all the atom pairs for which the nonbonded repulsions or the ionic interactions are expected to be considerable.

Then the F_{xop} matrix defined in eq. (27) is derived for the perovskite type crystal as:

$$F_{xop} = \begin{bmatrix} 2K+8H+\frac{8}{3}f_2 & & & & & \\ -2K & 2K+4F & & & & \\ -4H & -2F & 4H+2F+2f_1 & & & \\ -4H & -2F & 0 & 4H+2F+2f_1 & & \\ -\frac{8}{3}f_2 & 0 & -2f_1 & -2f_1 & 4f_1+\frac{8}{3}f_2 & \end{bmatrix}, \quad (44)$$

where the basis coordinates are

$$[\Delta Z_{op}(1),\ \Delta Z_{op}(2),\ \Delta Z_{op}(3),\ \Delta Z_{op}(4),\ \Delta Z_{op}(5)] \quad (45)$$

or the corresponding coordinates for ΔX or ΔY. $\Delta Z_{op}(i)$ denotes the optically active Cartesian coordinate corresponding to the i-th atom (1:M; 2, 3, 4: F; and 5·K, see Fig 6). The eigenvalues (Λ) and eigenvectors (L_x) of the $M^{-1}F_{xop}$ matrix are calculated. Five eigenvalues corresponding to four f_{1u} and one f_{2u} vibrations are obtained, one eigenvalue of the f_{1u} species corresponding to the acoustical (translational) mode being zero. The calculated frequencies are listed in Table 4, together with the observed frequencies.

TABLE 4

CALCULATED AND OBSERVED FREQUENCIES IN CM^{-1} OF THE PEROVSKITE FLUORIDES KMF_3 (M Ni, Mg AND Zn).

	$KNiF_3$		$KMgF_3$		$KZnF_3$	
	Calc	*Obs*[a]	*Calc*	*Obs*[b]	*Calc*	*Obs*
$\nu_1(f_{1u})$	455	446	477	478	435	430
$\nu_2(f_{1u})$	250	255	285	300	225	206
$\nu_3(f_{1u})$	144	153	160	156	134	142
$\nu_4(f_{2u})$	214	ia	234	ia	196	ia[c]

[a] Reflection data (Perry)[9]: 445, 245, 153.
[b] Reflection data (Perry)[9]: 450, 295, 140
[c] ia, inactive in the infrared spectrum.

The values of force constants are given in Table 5. These values were determined as follows. Among the five potential constants in eq. (43), F is estimated from the nonbonded fluorine–fluorine interaction potential of the Lennard–Jones 6–12 type which were studied in detail for organic compounds[17] such as CF_4, SiF_4

TABLE 5

FORCE CONSTANTS IN md/Å OF THE PEROVSKITE FLUORIDES KMF_3

	$KNiF_3$	$KMgF_3$	$KZnF_3$
K(M—F)	0 80	0 60	0 75
H(FMF)	0 063	0.083	0 038
F(F F)	0 05	0 05	0 05
$f_1(K^+ \quad F^-)$	0 09	0 09	0 09
$f_2(K^+ \cdot M^{2+})$	0 03	0 03	0 03

and BF_3. The values of f_1 and f_2 are assumed to be of the same value for $KNiF_3$, $KMgF_3$ and $KZnF_3$, since the distances q' and q^* are almost the same for all of them. The values of f_1 and f_2 are determined to obtain a good fit for the ν_3 frequencies of these salts, because they contribute mainly to the ν_3 frequency. Then for each fluoride, K and H are calculated to get good agreement between the observed and calculated frequencies. The elements of the F_{xop} matrix are the values of the force constants (in md/Å) in terms of Cartesian coordinates given in eq. (45). For $KNiF_3$, they are

$$F_{xop}(KNiF_3) = \begin{bmatrix} 2\,18 & & & & \\ -1.60 & 1.80 & & & \\ -0.25 & -0.10 & 0\,53 & & \\ -0.25 & -0.10 & 0 & 0.53 & \\ -0.08 & 0 & -0\,18 & -0.18 & 0\,44 \end{bmatrix} \tag{46}$$

There remains the problem of whether there is another set of force constants which could explain the observed frequencies. However, with the restriction that the stretching force constant K should be larger than the bending force constant H as well as the interaction constants f_1 and f_2, only one set of force constants, shown in Table 5, is obtained, from the observed frequencies.

The displacement of each atom for each mode may be sketched on the basis of the eigenvectors (L_x: eq. (28)). An approximate (mass-adjusted) displacement of each atom in the crystal $KNiF_3$, is given as an example in Fig. 8, on the basis of the calculated values of the matrix elements of the $M^{\frac{1}{2}}L_x$ matrix shown in Table

TABLE 6

MASS-ADJUSTED L_x MATRIX ELEMENTS OF $KNiF_3$

	Q_1 455	Q_2·250	Q_3:144	Q_4·218
$\sqrt{m_{Ni}}\Delta Z_1$ (Ni)	−0 49	−0 36	−0 50	0
$\sqrt{m_F}\Delta Z_2$ (F)	+0 87	−0.18	−0 29	0
$\sqrt{m_F}\Delta Z_3$ (F)	−0 01	+0 61	+0 00	−0.71
$\sqrt{m_F}\Delta Z_4$ (F)	−0 01	+0.61	+0 00	+0 71
$\sqrt{m_K}\Delta Z_5$ (K)	+0 01	−0 29	+0 81	0

$Z_i = (1/N)\,\Sigma\Delta z_i$

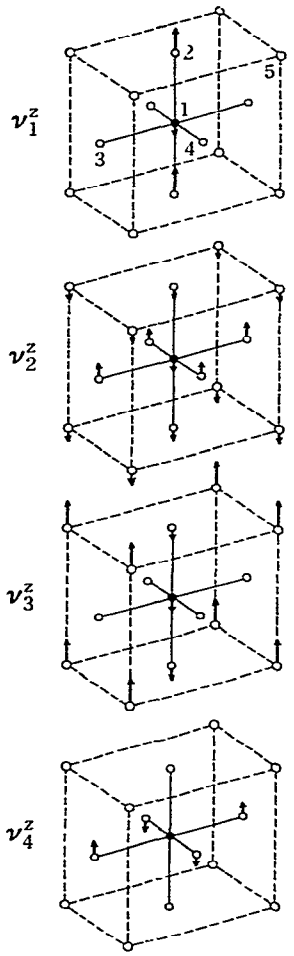

Fig 8. Displacements of each atom for the lattice vibrations in $KNiF_3$ (based on mass-adjusted L_x matrix elements)

6. It can be seen that the ν_1 mode is a pure Ni–F stretching mode of the NiF_6-octahedron with a negligible amount of K^+ ion displacements and the ν_2 mode is nearly a Ni–F bending mode with small displacements of K^+ ions. The ν_3 mode may be designated as a K-NiF_3 lattice mode but it should be noted that the displacements of F(3) and F(4) are negligible.

The lattice vibrations of the rutile fluorides will be discussed briefly next, since its analysis is useful to confirm the vibrational assignments of the perovskite fluorides. The rutile fluoride such as NiF_2 has a tetragonal structure with the space group $D_{4h}{}^{14}$. The Bravais primitive cell consists of two molecules of NiF_2, *i.e.*, two Ni's (1 and 2) and four F's (3, 4, 5, and 6), as shown in Fig. 9. Optically active lattice vibrations are

$$1a_{1g} + 1a_{2g} + 1b_{1g} + 1b_{2g} + 1e_g + 1a_{2u} + 2b_{1u} + 3e_u$$

of which the $1a_{2u}$ and $3e_u$ modes are infrared active. The Cartesian displacements of these lattice vibrations are as follows:

$$a_{1g} : (X_s)_1 = \tfrac{1}{2}\Delta(X_3 - X_4 - Y_5 + Y_6),$$
$$a_{2g} : (X_s)_2 = \tfrac{1}{2}\Delta(Y_3 - Y_4 + X_5 - X_6),$$
$$b_{1g} : (X_s)_3 = \tfrac{1}{2}\Delta(X_3 - X_4 + Y_5 - Y_6),$$
$$b_{2g} : (X_s)_4 = \tfrac{1}{2}\Delta(Y_3 - Y_4 - X_5 + X_6),$$
$$e_g : (X_s)_5 = (\tfrac{1}{2})^{\frac{1}{2}}\Delta(Z_3 - Z_4); (\tfrac{1}{2})^{\frac{1}{2}}\Delta(Z_5 - Z_6),$$

a_{2u} : a linear combination of

$$(X_s)_6 = (\tfrac{1}{2})^{\frac{1}{2}}\Delta(Z_1 + Z_2),$$
$$(X_s)_7 = \tfrac{1}{2}\Delta(Z_3 + Z_4 + Z_5 + Z_6),$$

b_{1u} : linear combinations of

$$(X_s)_8 = (\tfrac{1}{2})^{\frac{1}{2}}\Delta(Z_2 - Z_3),$$
$$(X_s)_9 = \tfrac{1}{2}\Delta(Z_3 + Z_4 - Z_5 - Z_6),$$

e_u : linear combinations of

$$(X_s)_{10} = \Delta X_1; \Delta Y_1,$$
$$(X_s)_{11} = \Delta X_2; \Delta Y_2,$$
$$(X_s)_{12} = (\tfrac{1}{2})^{\frac{1}{2}}\Delta(X_3 + X_4); (\tfrac{1}{2})^{\frac{1}{2}}\Delta(Y_3 + Y_4,)$$
$$(X_s)_{13} = (\tfrac{1}{2})^{\frac{1}{2}}\Delta(X_5 + X_6); (\tfrac{1}{2})^{\frac{1}{2}}\Delta(Y_5 + Y_6).$$

A calculation of the optically active lattice frequencies was made by using the potential constants transferred from the perovskite fluorides discussed above. Although the potential field which governs the rutile fluoride is not exactly the same as that for the NiF_6-octahedral part in the perovskite fluoride, the same values of the Ni–F stretching (K) and F–Ni–F bending (H) force constants were assumed. The purpose of the calculation is to confirm the vibrational assignment of the perovskite fluoride and also to learn the approximate modes of lattice vibrations of a rutile type crystal. The repulsive constants F(F···F) were adjusted according to the fluorine–fluorine distances q(F ··F). The results of the calculation on the basis of the above approximate values of force constants are shown in Table 7 and compared with the observed frequencies obtained by Balkanski *et al.*[10] and Perry *et al.*[9]. The agreement between the observed and calculated frequencies in Table 7 is satisfactory, when considering that in the present approach the M–F stretching and bending force constants of the KMF_3 were transferred to the rutile counterpart without any modification. This result provides further evidence for the vibrational assignments of the perovskite fluoride. An approximate displacement of each atom in the crystal is given in Fig. 9, from which the $\nu_6(a_{2u})$ and $\nu_9(e_u)$ around 400 cm^{-1} may be designated as the M–F stretching mode and the $\nu_{10}(e_u)$ and $\nu_{11}(e_u)$ around 250 cm^{-1} as the M–F bending mode. A comparison

TABLE 7

LATTICE VIBRATION FREQUENCIES IN CM^{-1} OF THE RUTILE FLUORIDES MF_2

	NiF_2		MgF_2		ZnF_2	
	Obs.[9 10]	*Calc*	*Obs* [9 10 19]	*Calc.*	*Obs* [9,10 19]	*Calc.*
$\nu_1(a_{1g})$. R[a]	—	481	410	389	350	395
$\nu_2(a_{2g})$. ia[b]	—	288	—	319	—	244
$\nu_3(b_{1g})$ R	—	444	515	417	522	423
$\nu_4(b_{2g})$. R	—	68	92	76	70	58
$\nu_5(e_g)$: R	—	330	295	303	253	314
$\nu_6(a_{2u})$ IR[c]	370	421	399	489	294	385
$\nu_7(b_{1u})$: ia	—	414	—	454	—	389
$\nu_8(b_{1u})$· ia	—	164	—	233	—	133
$\nu_9(e_u)$· IR	439	447	450	477	380	421
$\nu_{10}(e_u)$. IR	287	254	410	358	244	215
$\nu_{11}(e_u)$ IR	227	215	247	261	173	186

[a]) R, Raman active [b] ia) inactive in the infrared spectrum. [c]) IR, infrared active

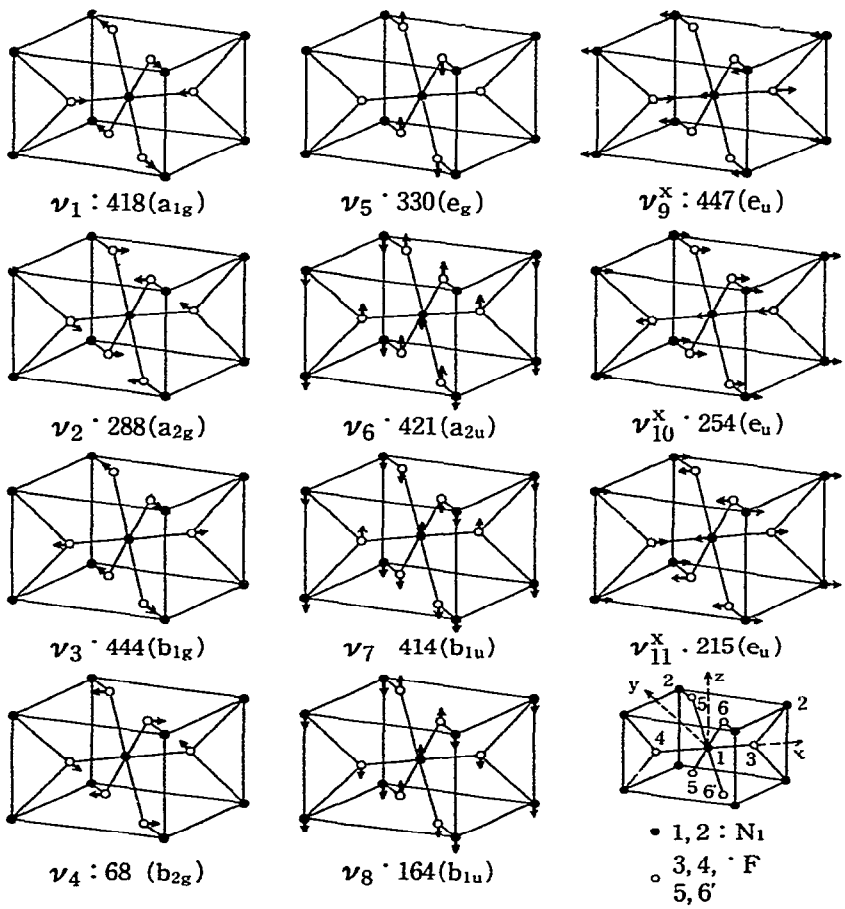

Fig 9. Displacements of each atom for the lattice vibrations in NiF_2 (based on mass-adjusted L_x matrix elements).

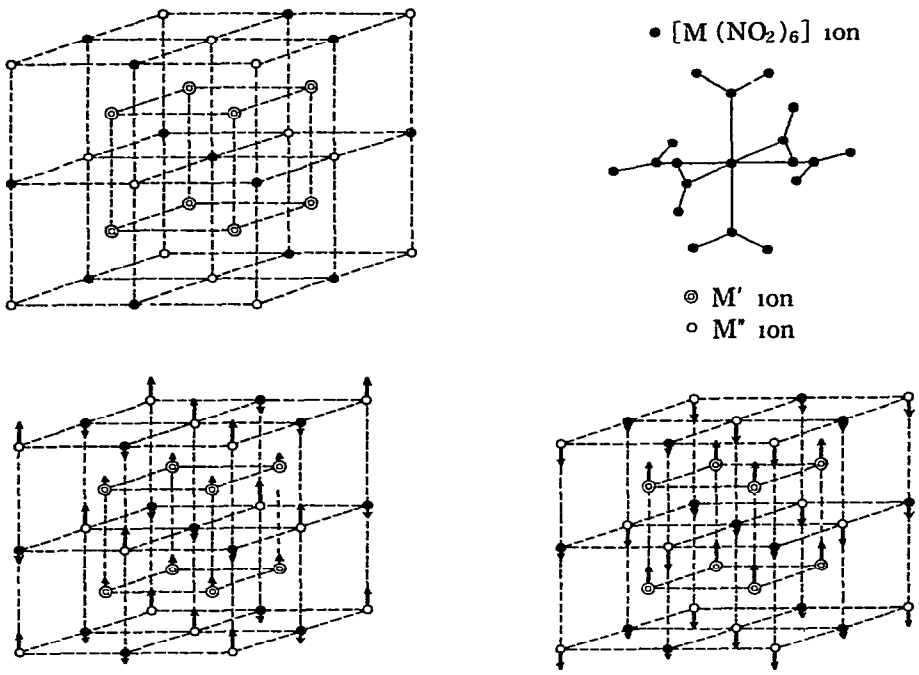

Fig 10. Structure of hexanitro-complex salts with the space group T_h^3 and approximate modes of lattice vibrations ν_9 and ν_{10}

of the calculated frequencies of g-species with the observed Raman frequencies obtained by Porto *et al.*[19] is also given in Table 7

(*ii*) *Hexanitrocomplex salts*

Complex salts particularly suitable for the study of the interaction between complex ion and outer ion are hexanitrocomplex salts. The crystal structure of $M_3[Co(NO_2)_6]$ (M:K, Rb and Cs) and $K_2M[Ni(NO_2)_6]$ (M:Ca and Ba) is cubic with the space group T_h^3 as shown in Fig. 10. The Bravais primitive cell consists of 22 atoms; one complex ion (19 atoms) and three cations. The result of the factor group analysis performed according to the procedure described in section (B, *iv*) is given in Table 8, from which ten vibrations of the f_{1u} species are expected to be observed in the infrared. The far infrared spectra are given in Fig. 11. The bands become sharp and shift to higher frequency with a lowering of temperature[21].

The spectra of $M_3[Co(NO_2)_6]$ shown in Fig 11(a) reveal six bands in the region below 500 cm^{-1} and in the higher frequency region not shown here there are four bands, corresponding to the NO_2 symmetric and antisymmetric stretching, NO_2 scissoring, and NO_2 wagging modes (see Table 10 below). Therefore, the

TABLE 8

FACTOR GROUP ANALYSIS OF $M_3[Co(NO_2)_6]$ (K, Rb, AND Cs)[a] AND $K_2M[Ni(NO_2)_6]$ (M:Ca AND Ba)

T_h^3	N	T	T'	R'	n	
A_g	3	0	0	0	3	R
A_u	1	0	0	0	1	ia
E_g	3	0	0	0	3	R
E_u	1	0	0	0	1	ia
F_g	7	0	1	1	5	R
F_u	11	1	2	0	8	IR

[a] Symbols N, number of the total freedoms, T, number of the acoustical translational motions, T', number of the optical translational lattice vibrations; R', number of the rotational lattice vibrations, n, number of the intramolecular vibrations of $[Co(NO_2)_6]^{3-}$ ion, R, Raman active, IR, infrared active, ia, inactive

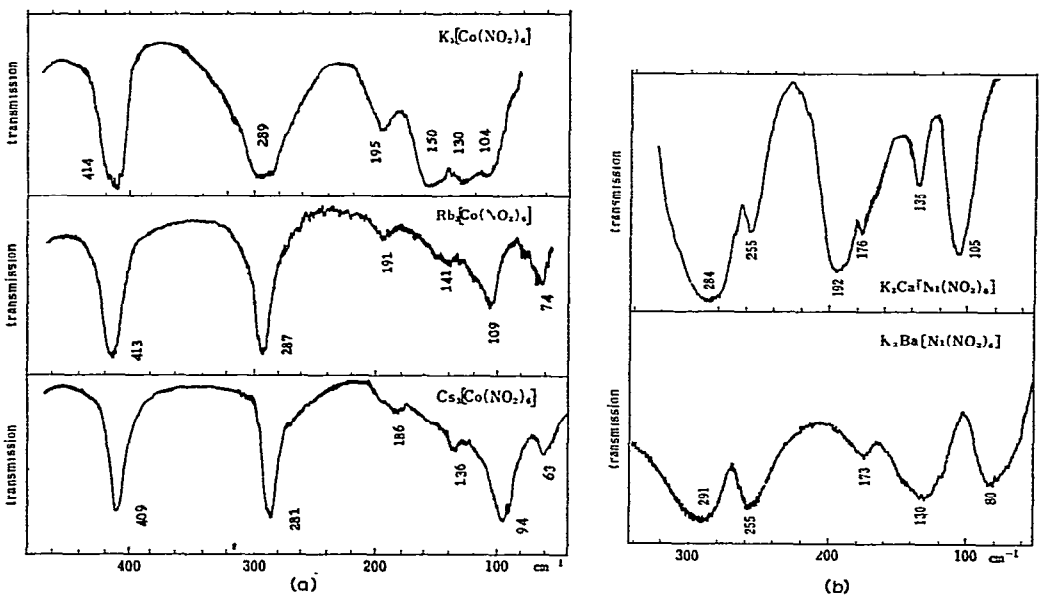

Fig. 11 Far infrared spectra of hexanitro-complex salts at room temperature (samples dispersed in polyethylene sheet 3–5 mg/cm²).
(a) $M_3[Co(NO_2)_6]$ (M:K, Rb and Cs), (b) $K_2M[Ni(NO_2)_6]$ (M.Ca and Ba).

total number of the observed infrared bands is ten as expected in Table 8. In the region below 150 cm^{-1} are observed two bands for which there is an appreciable dependence of the frequencies with the outer cations (132, 109 and 94 cm^{-1}; and 106, 74 and 63 cm^{-1}, for K, Rb and Cs salts, respectively) These two bands are interpreted to arise mainly from lattice vibrations due to the interaction between the complex ion and the outer cations. In a similar manner, the spectra of $K_2M[Ni(NO_2)_6]$ are plausibly explained on the basis of the T_h^3 structure. However, the intramolecular vibrations of the complex ion in the low frequency

TABLE 9

INTRAMOLECULAR POTENTIAL CONSTANTS (md/Å) FOR $[Co(NO_2)_6]^{3-}$ AND $[Ni(NO_2)_6]^{4-}$*

	$[Co(NO_2)_6]^{3-}$	$[Ni(NO_2)_6]^{4-}$
F_{dia}(MN str) md/Å	1.50	0 80
F_{dia}(NO str) md/Å	9.30	9 30
F_{dia}(NMN def) md Å	1.10	0 60
F_{dia}(ONO def) md Å	1.78	2 00
F_{dia}(MNO def) md Å	0 50 0 30 (Na salt)	0 40
F_{dia}(NO_2 wag) md·Å	0 55	0 32
F_{dia}(NO_2 twist) md·Å	0 03 (assumed)	0 03
F(N ·N) md/Å	0 05	0 20**
F(O ·O) md/Å	3.00	3.00
F(M ·O) md/Å	0 20	0 10
p(NO, NO) md/Å	0 50	0 50

* In the Urey–Bradley approach, diagonal elements of the F-matrix corresponding to the bond stretching modes include F as well as K and those for angle deformation modes include F as well as H The off-diagonal elements are expressed in terms of F

** Taking into account the appreciable interaction between the Ni–N stretching and NMN deformation modes, the effective value of F(N N) was assumed to be large[22f].

region are more or less coupled with the lattice vibrations. A normal coordinate analysis is needed for a further discussion about this problem.

The optically active vibration frequencies of the crystal are calculated for the above complex salts according to the procedure described in section (B, ii), by using the potential function

$$V = V_{intra} + V_{inter} \tag{47}$$

where V_{intra} and V_{inter} denote the intramolecular potential in the complex ion and the interionic interaction potential between the complex ion and the outer cations, respectively. For the intramolecular potential, the modified Urey–Bradley force field (MUBFF) has been used and the use of this type of potential in the vibrational analysis of the complex ions has been fully discussed in the several papers[22] published in our laboratory and so there will be no further discussion here. The force constants used are listed in Table 9, where K, H, and F denote the bond stretching, the angle bending, and the repulsion between nonbonded atoms, respectively. F_{dia} means the diagonal element of the F matrix (potential energy matrix) for the corresponding mode. p(NO, NO) is the resonance interaction constant. The value of p(MN, MN) cannot be determined unless the frequencies of the g-species are available. For the interaction potential, it is assumed that this term arises from the interaction between the M^+ ions and the neighboring O atoms[23]. For these complex salts the nearest and the second nearest $M^+ \cdots O$ distances are 2.80–3.15 Å ($q_2(M'' \cdots O)$) and 3.05–3.30 Å ($q_1(M' \cdots O)$, respectively (see Fig. 12 and Table 10 below). The interaction between the atoms whose distances are longer than 3.5 Å is not taken into consideration.

TABLE 10 (a)

OBSERVED AND CALCULATED FREQUENCIES (CM^{-1}) OF $M_3[Co(NO_2)_6]$ SALTS

T_h^3 / F_u	$K_3[Co(NO_2)_6]$ Obsd	$K_3[Co(NO_2)_6]$ Calcd	$Rb_3[Co(NO_2)_6]$ Obsd	$Rb_3[Co(NO_2)_6]$ Calcd	$Cs_3[Co(NO_2)_6]$ Obsd	$Cs_3[Co(NO_2)_6]$ Calcd	*Vib modes*
ν_1	1386	1393	1399	1393	1400	1393	NO_2 antisym str
ν_2	1332	1325	1327	1325	1326	1325	NO_2 sym str
ν_3	827	818	827	818	832	817	NO_2 scissor
ν_4	637	619	633	619	630	618	NO_2 wag
ν_5	416	421	413	421	409	420	Co–N str
ν_6	293	293	287	288	281	286	NO_2 rock and skel def
ν_7	195	201	191	181	186	170	skel def and M′ lattice
ν_8	154	157	141	149	136	141	skel def, NO_2 rock, and M″ lattice
ν_9	132	162	109	117	94	95	M″ and M′ lattice
ν_{10}	106	106	74	76	63	59	M′ and M″ lattice

Interionic potential constants and interatomic distances of $M_3[Co(NO_2)_6]$ salts

	K^+ O	Rb^+ O	Cs^+ O
f_1, md/Å	0 11	0 10	0 08
q_1, Å	3 05	3 15	3 30
f_2, md/Å	0.14	0 12	0 10
q_2, Å	2 83	2 95	3.15

TABLE 10 (b)

OBSERVED AND CALCULATED FREQUENCIES (CM^{-1}) OF $K_2Ca[Ni(NO_2)_6]$ AND $K_2Ba[Ni(NO_2)_6]$

T_h^3 / F_u	$K_2Ca[Ni(NO_2)_6]$ Obsd	Calcd	*Vib modes*	$K_2Ba[Ni(NO_2)_6]$ Obsd	Calcd	*Vib modes*
ν_1	1355	1388	NO_2 antisym str	1343	1387	NO_2 antisym str
ν_2	1325	1325	NO_2 sym str	1306	1325	NO_2 sym str
ν_3	834	838	NO_2 scissor	838 (813)	837	NO_2 scissor
ν_4	458	461	NO_2 wag	433	460	NO_2 wag
ν_5	284	306	Ni–N str and NO_2 rock and wag	291	304	Ni–N str and NO_2 rock and wag
ν_6	255	244	NO_2 rock and Ca lattice	255	230	NO_2 rock and skel def
ν_7	192	196	K lattice and skel def	173	180	K lattice and skel def
ν_8	176	154	Ca lattice and skel def	130	132	skel def and K lattice
ν_9	135	140	skel def and NO_2 rock	(130)	107	skel def and NO_2 rock
ν_{10}	105	94	Ca and K lattice and skel def	80	73	Ba lattice

Interionic potential constants and interatomic distances

	$K_2Ca[Ni(NO)_{26}]$ $K^+\cdots O$	Ca^{2+} O	$K_2Ba[Ni(NO_2)_6]$ $K^+\cdots O$	$Ba^{2+}\cdot O$
f_1, md/Å	0.12		0.10	
q_1, Å	3 01		3.13	
f_2, md/Å		0.15		0 12
q_2, Å		2 77		2 93

The calculated and observed frequencies and the interionic potential constants are shown in Table 10. It can be seen that the observed bands for this series of complex salts are satisfactorily explained by the above potential function and by use of the interionic potential constants $f(M^+ \cdots O)$ of *ca.* 0.1 md/Å, which change slightly with the interatomic distances.

A sketch for the approximate motion for $M_3[Co(NO_2)_6]$ is given in Fig. 10, on the basis of the calculated eigenvectors ($M^{\frac{1}{2}}L_x$). It is seen that M′ and M″ displace in the same direction for the ν_9 mode and in the opposite direction for the ν_{10} mode, though in the ν_9 vibration for the K and Rb salts the lattice modes are coupled considerably with the intramolecular modes For the $K_2M[Ni(NO_2)_6]$ salts, the vibrations below 200 cm^{-1} exhibit very complicated modes in which lattice modes of K^+ and M^{2+} ions and intramolecular deformation modes are mixed in a complex manner. Approximate modes are described in Table 10.

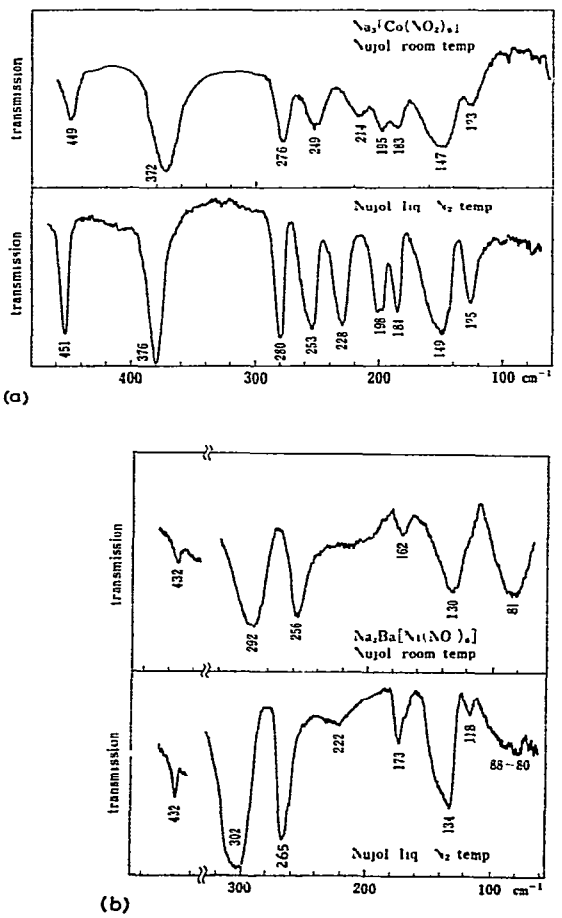

Fig. 12. Low-temperature far infrared spectra of $Na_3[Co(NO_2)_6]$ (a) and $Na_2Ba[Ni(NO_2)_6]$ (b).

Next the spectra of $Na_3[Co(NO_2)_6]$ and $Na_2Ba[Ni(NO_2)_6]$ shown in Fig. 12 will be discussed. The crystal structure of these Na salts has not been determined. The spectrum of $Na_3[Co(NO_2)_6]$ is quite different from those for $M_3[Co(NO_2)_6]$ (M:K, Rb and Cs)[21,24]. The complicated spectrum of the Na salt will be explained on the basis of a structure with a lower symmetry for the $[Co(NO_2)_6]^{3-}$ ion, the C_{3i} structure where the NO_2 plane rotates about the Co–N axis. This C_{3i} structure may be understood by the smaller ionic radius of the Na^+ ion, since for the T_h structure four interatomic distances q_1 (Na′···O) in Fig. 13, are too large to form a stable crystal. When the $[Co(NO_2)_6]^{3-}$ ion takes a C_{3i} structure, two of the q_1(Na′···O) distances become shorter and a stable crystal may be formed (see Fig. 13).

In order to see whether this C_{3i} structure may explain the lattice frequencies as well as the intramolecular vibration frequencies for the Na salt, optically active

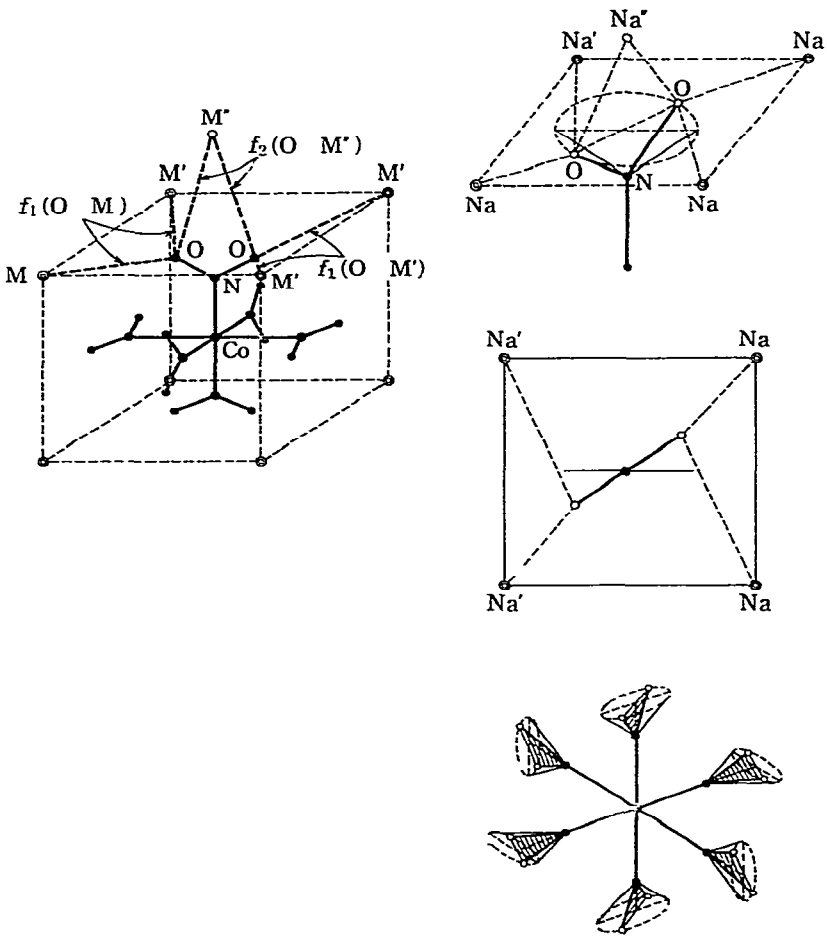

Fig 13 Positions of oxygen atoms and outer cations for $M_3[Co(NO_2)_6]$ (M K, Rb and Cs) and $Na_3[Co(NO_2)_6]$, and structure of $[Co(NO_2)_6]^{3-}$ in the Na salt

TABLE 11

FACTOR GROUP ANALYSIS OF $Na_3[Co(NO_2)_6]$*

C_{3i}	N	T	T'	R'	n	
A_g	10	0	1	1	8	R
A_u	12	1	2	0	9	IR
E_g	10	0	1	1	8	R
E_u	12	1	2	0	9	IR

* See Table 8 for the meanings of N, T, T', R', n, R, and IR.

vibration frequencies of the crystal were calculated. It is considered that Na^+ cations and Co atoms are located at the lattice points as shown in Fig. 10 as in the case of a cubic crystal. However, owing to the twisting of the NO_2 plane, the crystal structure is no longer cubic. On the basis of the C_{3i} structure with a twisting angle of 30° and a = 10.00 Å, the interatomic distances q(Na···O) are calculated as: q_1(Na′···O) = 2.55 Å, q_1'(Na′...O) = 3.42 Å, and q_2(Na″· ·O) = 2.62 Å (see Fig. 13).

The result of the factor group analysis is shown in Table 11, from which both A_u and E_u vibrations are expected to appear in the infrared. The calculated frequencies are given in Table 12, together with the interionic potential constants. In this calculation the intramolecular force constants are the same as those for

TABLE 12

CALCULATED AND OBSERVED FREQUENCIES (cm^{-1}) OF $Na_3[Co(NO_2)_6]$

A_u	*Calcd*	*Vib modes*	E_u	*Calcd*	*Vib modes*	*Obsd*
ν_1	1389	NO_2 antisym str	ν_1'	1391	NO_2 antisym str	1425
ν_2	1324	NO_2 sym str	ν_2'	1324	NO_2 sym str	1333
ν_3	802	NO_2 scissor	ν_3'	801	NO_2 scissor	845, 831
ν_4	662	NO_2 wag	ν_4'	630	NO_2 wag	623
ν_5	382	Co–N str	ν_5'	441	Co–N str	449, 372
ν_6	270	NO_2 rock and skel def	ν_6'	283	NO_2 rock and Na″ lattice	276, 249
ν_7	219	Na″ lattice	ν_7'	237	Na′ and Na″ lattice	214
ν_8	179	skel def and Na′ and Na″ lattice	ν_8'	194	Na″ lattice and NO_2 rock	195, 183
ν_9	163	skel def and Na′ and Na″ lattice	ν_9'	158	skel def and Na′ and Na″ lattice	147
ν_{10}	109	Na′ lattice and skel def	ν_{10}'	133	skel def	123
ν_{11}	94	NO_2 twist	ν_{11}'	94	NO_2 twist	.

Interionic potential constants and interatomic distances

(Na^+ O) *Constant*	*Value, md/Å*	*Distance*	*Value, Å*
f_1	0 15	q_1	2 55
f_1'	0 05	q_1'	3 42
f_2'	0.15	q_2	2.62

the K, Rb, and Cs salts. It can be seen from Table 12 that the calculated frequencies for the C_{3i} crystal structure correspond with the observed frequencies of $Na_3[Co(NO_2)_6]$.

In the spectrum of $Na_3[Co(NO_2)_6]$, each band shifts to the higher frequency side by 2–5 cm^{-1} with a lowering of temperature. Among them a remarkable frequency shift and an intensity enhancement are seen for the band at 214 cm^{-1}. The reason for this feature is not certain. According to the calculation shown in Table 12, this band is assigned to the lattice vibration where the Na^+ ion displaces primarily. In the spectrum of $Na_2Ba[Ni(NO_2)_6]$ shown in Fig. 12(b), the band around 200 cm^{-1} behaves in a similar manner, which suggests that this band may be assigned to the lattice mode related to the Na^+ ion. The lowest band around 80 cm^{-1} of $Na_2Ba[Ni(NO_2)_6]$ may be assigned to the lattice mode related to the Ba^{2+} ion, since a similar band is observed in the spectrum of $K_2Ba[Ni(NO_2)_6]$.

(iii) Lattice vibrations of A'_2A'' C type cubic crystal (Hexanitro- and hexammine-complex salts)

If a hexanitrocomplex ion is regarded as one unit in Fig. 10, an A'_2A'' C type cubic crystal (C: complex ion) is formed. There are many hexanitrocomplex salts belonging to this type of cubic structure, some of which have been discussed in the preceding section (D, ii). Hexammine complex salts such as $[Co(NH_3)_6]Cl_3$ and $[Ni(NH_3)_6]Cl_2$ also belong to this type of cubic structure (A': Cl^-, A'': Cl^- and C: $[Co(NH_3)_6]^{3+}$ for the former; and A': Cl^-, A'': none and C: $[Ni(NH_3)_6]^{2+}$ for the latter). Since such a thorough normal coordinate analysis of complex salts as described in the preceding sections is not always possible, an approximate analysis of the lattice vibrations on the basis of the above simplified model is needed and worth while investigating. Though the low-frequency inner vibrations in the complex ion are somewhat coupled with the lattice vibrations as has been discussed in the previous section, the above approximate analysis neglects the coupling effect and estimates the intrinsic (uncoupled) lattice frequencies.

Consider an interionic potential as[25]:

$$V = \tfrac{1}{2}\sum f_1(\Delta q_1(A'\cdots C))^2 + \tfrac{1}{2}\sum f_2(\Delta q_2(A''\cdots C))^2 + \tfrac{1}{2}\sum f_3(\Delta q_3(A'\cdots A''))^2 . \tag{48}$$

According to the procedure in section (B, ii), the following secular equation to calculate two infrared active lattice vibration frequencies is finally obtained:

$$\begin{vmatrix} (8/3)f_1\mu_0+(4/3)f_1\mu-\lambda & (4\sqrt{2}/3)\,\mu_0 f_1 \\ 2\sqrt{2}f_2\mu_0 & 2f_2\mu_0+2f_2\mu'-\lambda \end{vmatrix} = 0 \tag{49}$$

where μ_0, μ and μ' denote the reciprocal masses of C (complex ion), A' and A'', respectively. If the force constant f_3, the interaction between A' and A'', is assumed to be zero, the two force constants $f_1(A'\cdots C)$ and $f_2(A''\cdots C)$ may be

determined by using the two observed lattice frequencies. The calculation has been made by use of the common values of f_1 and f_2 among $M_3[Co(NO_2)_6]$ and $M'_2M''[Ni(NO_2)_6]$ and the result is given in Table 13. The eigenvectors for the secular equation (49) show that for the higher vibration the M' and M'' ions displace in the same direction while for the lower one in the opposite direction, corresponding to ν_9 and ν_{10} shown in Fig. 10, respectively. The values of these force constants f_1 and f_2 are somewhat effective though artificial, however, this approach is useful for estimating the intrinsic frequencies of the lattice vibrations when the intramolecular modes are not coupled with them. It is found in Table 13 that these frequencies are located in the region where the intramolecular deformation frequencies are also expected to appear.

TABLE 13

LATTICE VIBRATION FREQUENCIES (CM^{-1}) OF $M_3[Co(NO_2)_6]$ AND $M'_2M''[Ni(NO_2)_6]$ TREATED AS A'_2A'' C TYPE CUBIC CRYSTALS AND THE RELATED FORCE CONSTANTS (md/Å)

$Na_3[Co(NO_2)_6]$	180	144	$Na_2Ba[Ni(NO_2)_6]$	178	66
$K_3[Co(NO_2)_6]$	144	109	$K_2Ca[Ni(NO_2)_6]$	143	108
$Rb_3[Co(NO_2)_6]$	111	76	$K_2Ba[Ni(NO_2)_6]$	143	65
$Cs_3[Co(NO_2)_6]$	99	61			

force constants $f_1 = 0\ 28, f_2 = 0\ 13, f_3 = 0\ 00$

TABLE 14

LATTICE VIBRATION FREQUENCIES (CM^{-1}) OF $[Co(NH_3)_6]X_3$ AND $[Ni(NH_3)_6]X_2$

	$[Co(NH_3)_6]X_3$		$[Ni(NH_3)_6]X_2$
X = Cl	150	—	110
X = Br	117	—	90
X = I	104	55?	81

Hexammine complex salts of this type of cubic structure have been studied in this laboratory[26] and by Sacconi *et al.*[27]. The lattice frequencies are listed in Table 14. For $[Co(NH_3)_6]X_3$ two lattice vibrations should be observed, however, only one band is observed, even if an extremely concentrated sample is used for measurement. The reason for this is not certain but the observed band may correspond to the higher lattice vibration (ν_9 in Fig. 10), for which the change of the dipole moment may be expected to be larger. For $[Ni(NH_3)_6]X_2$, there is no X'' and so only one lattice vibration is expected in the infrared.

(*iv*) *Hexacyanocomplex salts*

As examples of complex salts with structures which are neither cubic nor tetragonal, the infrared spectra of the hexacyanocomplex salts, $K_3[Cr(CN)_6]$ and $Cs_3[Cr(CN)_6]$, will be discussed. These hexacyanocomplex salts have a monoclinic structure with space group C_{2h}^5 like $K_3[Fe(CN)_6]$, which has been already cited

in the previous section (B, iv) as an example for the general explanation of factor group analysis. The Bravais primitive cell is composed of two complex ions and six cations (see Fig. 4), and therefore band splitting of the inner vibrations in the complex ion may be expected. It is seen from the factor group analysis shown in Table 2 that 26 a_u and 25 b_u vibrations are infrared active, of which 8 a_u and 7 b_u vibrations correspond to the lattice modes Lattice vibrations may be observed below 200 cm^{-1}.

The infrared spectra of $K_3[Cr(CN)_6]$ and $Cs_3[Cr(CN)_6]$ are shown[28] in Fig. 14. Many bands are observed in this far infrared region below 500 cm^{-1}. With a lowering of temperature some of the bands split into several components. Most of the bands shift to the higher frequency side; the band around 200 cm^{-1} in K salt and the one around 170 cm^{-1} in Cs salt are notable, and they may be attributed to the lattice modes due to the displacement of the outer cations. In

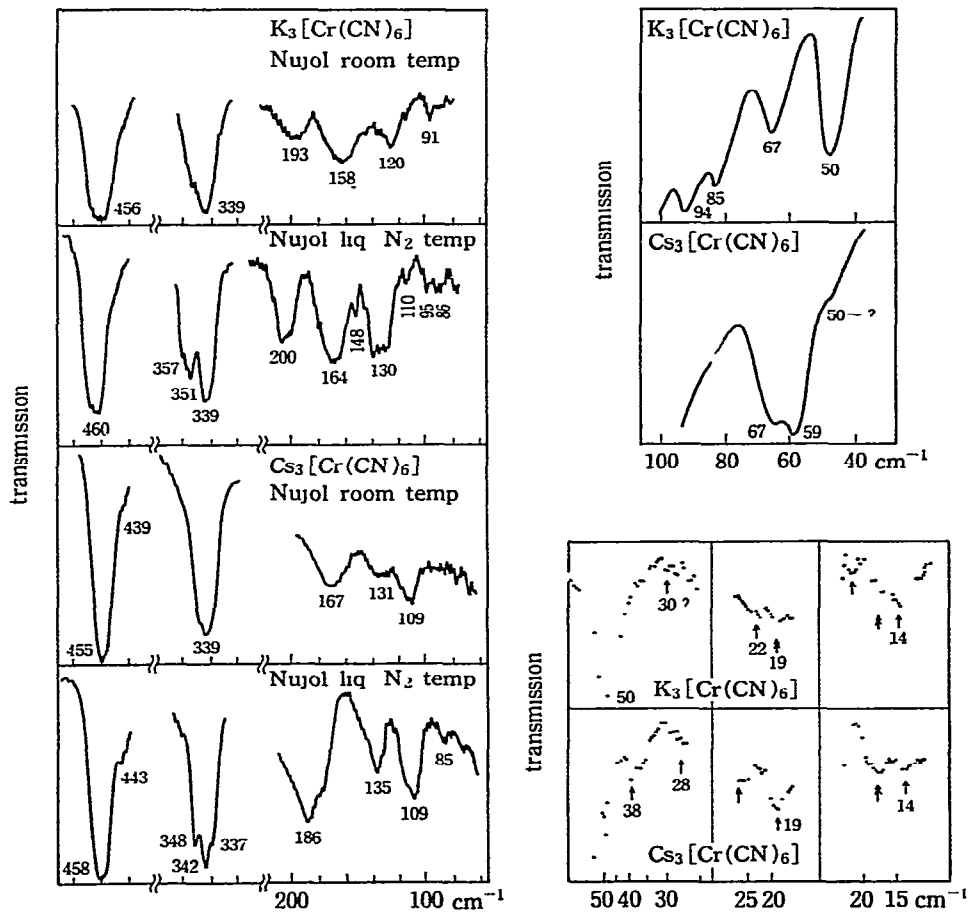

Fig. 14. Far infrared spectra of $K_3[Cr(CN)_6]$ and $Cs_3[Cr(CN)_6]$.

order to clarify how each inner vibration band splits in the spectrum of the crystal, the correlation of the point group of one complex ion, and the site group and factor group of the crystal, is given in Table 15. For an isolated complex ion, $[M(CN)_6]^{3-}$, only three modes (M–C stretching, M–C≡N bending and C–M–C deformation modes) of the f_{1u} species are expected in the infrared below 500 cm^{-1}. The C–M–C deformation frequencies are located below 200 cm^{-1} and they may be considerably coupled with the lattice modes. The band feature of the M–C≡N bending mode may be more complicated than that of the M–C stretching mode, since from the correlation table of Table 15 it is expected that the former mode has six components arising from both f_{1u} and f_{2u} species while the latter mode has three components arising from f_{1u} species (see Table 16). Therefore, the band around 450 cm^{-1} which does not show clearly splitting or multicomponents, may be assigned to the M–C stretching mode, while the band around 340 cm^{-1}, which splits into three or four components, may be assigned to the M–C≡N bending mode. The opposite interpretation was given by Jones for some $[M(CN)_6]^{n-}$ ions[29].

Optically active vibration frequencies were calculated for the structure given in Fig. 4 of the previous section (B, iv), which was determined by neutron diffraction (for $K_3[Co(CN)_6]$). The interionic potential constants for the atom pairs with the distances shorter than 4.0 Å are taken into consideration. First an estimate was made of the values of the interatomic or interionic potential constants depending upon their distances, referring to the relation given by Rittner and then these were modified so that the calculated frequencies may explain the observed fre-

TABLE 15

CORRELATION TABLE FOR REPRESENTATIONS OF $[M(CN)_6]^{3-}$ ION IN $K_3[M(CN)_6]$

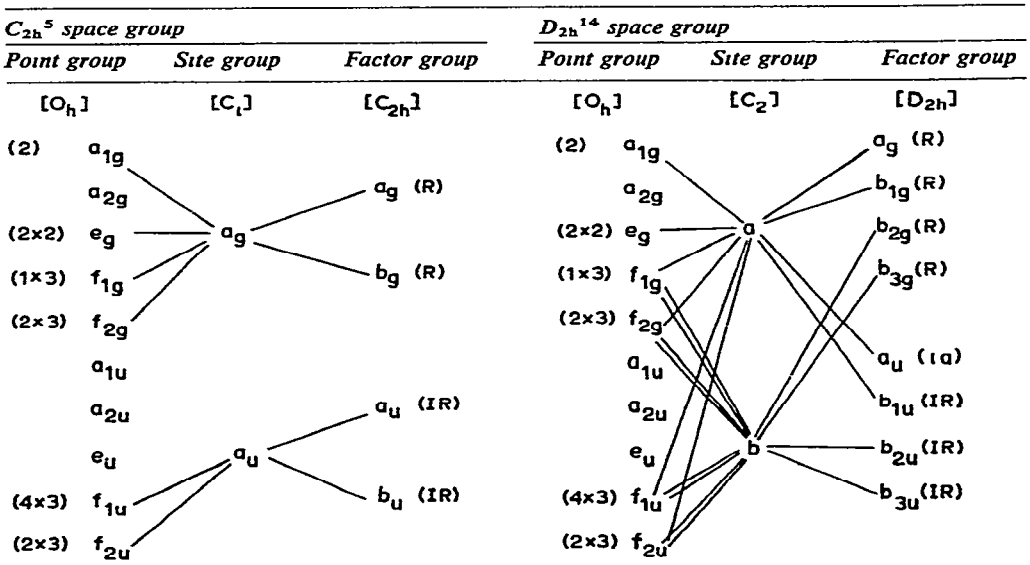

TABLE 16

OBSERVED (AT LOW TEMPERATURE) AND CALCULATED FREQUENCIES (cm^{-1}) OF $K_3[Cr(CN)_6]$ AND $Cs_3[Cr(CN)_6]$

$K_3[Cr(CN)_6]$			$Cs_3[Cr(CN)_6]$			$[Cr(CN)_6]^{3-}$	
obs.	*calc.* (b_u)	*calc.* (a_u)	*obs.*	*calc.* (b_u)	*calc.* (a_u)	*calc.*	*mode*
2121, 2119	2115, 2115, 2113	2115, 2115, 2113		2115, 2115, 2113	2115, 2115, 2113	2113 (f_{1u})	CN str
460	456, 454, 453	456, 454, 453	458, 443	456, 454, 453	456, 454, 453	452 (f_{1u})	MC str.
357, 351	365, 359, 358	365, 359, 358	348, 342	365, 359, 358	365, 359, 358	354 (f_{1u})	MCN bend.
339	345, 342, 338	345, 342, 338	337	345, 342, 338	345, 342, 338	336 (f_{2u})	
200	202, 189	203, 189	186	188, 179	188, 179		lattice
164	156	158	135	146, 126	146, 126	114 (f_{1u})	
130, 110	136, 121, 118	137, 124, 118	109	113, 107	113, 107	90 (f_{2u})	CMC def.
	105	108		91	92		
95	98	92	67, 59	70, 59	67, 59		
86, 67	84, 72, 67	81, 76, 60	50, 38	44, 39	45, 36		lattice
50, (30)	48, 24	47, 22	(23)	29	28		
(22, 19)		14	(19)	19	18, 10		
	calc. (a_g)	*calc* (b_g)		*calc.* (a_g)	*calc.* (b_g)	*calc*	
	2120, 2112, 2111	2120, 2112, 2111		2120, 2112, 2111	2120, 2112, 2111	2119 (a_{1g}) 2110 (e_g)	CN str.
	425, 420, 417	425, 420, 417		425, 420, 417	425, 420, 417	416 (f_{2g})	MCN bend.
	353	353		353	353	344 (a_{1g})	MC str
	309, 301	309, 301		308, 301	308, 301	295 (e_g)	
	261, 256, 245	261, 256, 245		261, 255, 245	261, 255, 245	242 (f_{1g})	MCN bend.
	189, 166	182, 174		177, 160	176, 162		lattice
	133, 104, 87	127, 110, 89		125, 99, 80	124, 101, 80	103 (f_{2g})	CMC def
	82, 62, 40, 8	80, 55, 40, 27		59, 40, 26, 6	59, 36, 24, 21		lattice

TABLE 17

POTENTIAL CONSTANTS USED IN THE CALCULATION

intramolecular force constants	
	$[Cr(CN)_6]^{3-}$
K(M—C) md/Å*	1 5
K(C=N) md/Å*	17 0
r_{MC}^2 H(CMC) md Å*	0 8
$r_{MC}r_{CN}$H(MCN) md Å*	0 16
F(C C) md/Å	0 15
p(MC_1, MC_2) md/Å	0 0
p(MC, CN) md/Å	0 4
interionic or interatomic potential constants	
$f(K^+ \cdot N)$ or $f(Cs^+ \quad N)$·	0.15 md/Å (for 2 5 Å)
	0 05 md/Å (for 2 9~3 0 Å)
	0 01 md/Å (for 3 8 Å)
$f(K^{+}\cdot\cdot C)$ or $f(Cs^{+}\cdot\cdot C)$:	0 04 md/Å (for 3 0~3.2 Å)
	0 02 md/Å (for 3 5 Å)

* diagonal elements of F-matrix for the internal coordinates

quencies as a whole. Of the intramolecular force constants, the stretching and deformation force constants corresponding to the diagonal matrix elements of the potential energy matrix (F-matrix) are adjusted so that a good fit between the observed and calculated frequencies may be obtained, while the repulsive force constants between the non-bonded atoms, corresponding to the off-diagonal F-matrix elements in the Urey–Bradley approach, were fixed as values derived from the intermolecular interactions of inert gases. The results of the calculations are listed in Table 16, together with the observed frequencies. This Table also includes the calculated frequencies for which the interionic force constants were assumed to be zero, from which the effect of the outer cations upon the inner vibrations in the complex ion is known. Table 17 gives the potential constants used for the calculation.

As a whole the observed frequencies correspond well with the calculated frequencies. For the monoclinic structure the metal ion is located at the center of symmetry and the "g" inner vibrations of the isolated complex ion correspond to the a_g and b_g species for the C_{2h}[5] crystal (see Table 15). Accordingly these vibrations may not be observed in the infrared spectrum. This is actually the case, since no band is observed in the region 340–200 cm^{-1}, where the a_g and b_g vibrations arising from the e_g and f_{1g} intramolecular vibrations of O_h point group exist. The band around 200 cm^{-1} of $K_3[Cr(CN)_6]$ is assigned to the lattice mode in which the K^+ ions displace primarily, on the basis of the eigenvector (L_x matrix). It is reasonable that the frequency of the corresponding band for the Cs salt is lower than that for the K salt. With temperature change this kind of lattice vibration is affected markedly. Several bands observed below 100 cm^{-1} are assigned to the lattice vibrations in which outer cations or complex ions as a

whole displace. The lattice vibrations due to the displacement of the $[M(CN)_6]^{3-}$ ion as a whole are located in the lower frequency region and are all translational lattice modes. Rotational lattice modes belong to a_g and b_g species and are not observed in the infrared spectrum.

A report that $K_3[Co(CN)_6]$ is polytypic with two unit cells predominating (one monoclinic and one orthorhombic) was given by Kohn and Townes[30]. In addition to the monoclinic structure with the space group $C_{2h}{}^5$ mentioned above, the orthorhombic structure with the space group $D_{2h}{}^{14}$ was found. The correlation table for the latter crystal structure is different from that for the former and is also given in Table 15. As seen from Table 15, the selection rule for the infrared spectrum is different and details will not be discussed here. The effect of "polytypism" on the infrared spectrum and lattice vibrations will be reported in a forthcoming paper from our laboratory. However, it can be seen that the infrared spectrum shown in Fig 14 of $K_3[Cr(CN)_6]$ and $Cs_3[Cr(CN)_6]$ is not consistent

TABLE 18

POTENTIAL CONSTANTS (md/Å) OBTAINED FROM INFRARED FREQUENCIES (CM^{-1})*

(a) *Force constants of the covalent bond*				
K(ClCl)	3 2		Cl_2	556
K(PtF)	4 75		PtF_6	705
(b) *Force constants of the coordination bond*				
(b1) *Halogeno complexes*[a]				
K(PtF)	3 07		$Cs_2[PtF_6]$	571
K(PtCl)	1 81		$K_2[PtCl_6]$	344
K(PdCl)	1 47		$K_2[PdCl_6]$	340
K(PtBr)	1 61		$K_2[PtBr_6]$	244
K(PtCl)	1 60		$K_2[PtCl_4]$	320
K(PdCl)	1.40		$K_2[PdCl_4]$	233
K(CoCl)	1.41		$[CoCl_2(NH_3)_4]Cl$	353
K(CoBr)	1 57		$[CoBr_2(NH_3)_4]Br$	318
(b2) *Ammine complexes*[b]				
K(PtN)	2 39		$[Pt(NH_3)_6]Cl_4 \cdot H_2O$	536
K($Co^{III}N$)	1 39		$[Co(NH_3)_6]Cl_3$	503
K(CrN)	1 25		$[Cr(NH_3)_6]Cl_3$	470
K(NiN)	0 65		$[Ni(NH_3)_6]Cl_2$	330
K($Co^{II}N$)	0 65		$[Co(NH_3)_6]Cl_2$	318
K(PtN)	2 22		$[Pt(NH_3)_4]Cl_2 \cdot H_2O$	510
K(PdN)	1 97		$[Pd(NH_3)_4]Cl_2 \cdot H_2O$	491
K(CuN)	1 17		$[Cu(NH_3)_4]SO_4$	420
(b3) *Nitro complexes*[c]				
K(CoN)	1 50		$K_3[Co(NO_2)_6]$	410
K(NiN)	0 80		$K_2Ca[Ni(NO_2)_6]$	286
(b4) *Cyano complexes*[d]				
K(CoC)	2.60		$K_3[Co(CN)_6]$	565
K(FeC)	2 10		$K_3[Fe(CN)_6]$	512
K(CrC)	1.50		$K_3[Cr(CN)_6]$	456
(b5) *Perovskite fluorides*[e]				
K(NiF)	0 80	(2 01 Å)	$KNiF_3$	446

K(MgF)	0 60	(1 99 Å)	$KMgF_3$	:	478
K(ZnF)	0 75	(2 03 Å)	$KZnF_3$	:	430
(b6) *Metal oxides*[f]					
K(NiO)	: 0 75	(2.10 Å)	NiO	:	460
K(FeO)	: 0.62	(2.15 Å)	FeO	:	410
K(CoO)	: 0 65	(2.12 Å)	CoO	:	420
(c) *Force constants in the inorganic crystals*[g]					
K(CaF)	: 0.31	(2.35 Å)	CaF_2	:	322
K(CeO)	: 0 69	(2 34 Å)	CeO_2	:	345
K(ThO)	. 0 83	(2 42 Å)	ThO_2	:	365
K(ZnO)*	: 0 70	(1.95 Å)	ZnO	:	380
K(CdS)*	: 0 60	(2 52 Å)	CdS	:	228
(* taken into account the polarization forces)					
(d) *Force constants in the ionic crystals*[h]					
NaCl	: 0.11_2	(2 82 Å)			
NaBr	: $0\ 10_3$	(2 98 Å)			
KCl	. 0.11_5	(3 15 Å)			
KBr	: 0.11_5	(3.30 Å)			
KI	: $0\ 09_3$	(3 53 Å)			
CsCl	. $0\ 08_6$	(3 57 Å)			
CsBr	: $0\ 09_9$	(3.71 Å)			
CsI	: $0\ 08_3$	(3.95 Å)			
(e) *Interionic and interaction potential constants*[i]					
$f(K^+ \cdot\cdot Cl^-)$	0 045	(3 44 Å)	$K_2[PtCl_6]$	:	90
$f(K^{+}\cdot\cdot Cl^-)$	. 0 115	(3 22 Å)	$K_2[PtCl_4]$	:	110
$f(Na^{+}\cdot\cdot O)$	: 0 15	(2 6 Å~)			
	: 0.05	(3 4 Å~)			
$f(K^+ \cdot O)$	: 0.14	(2 83 Å)	$M_3[Co(NO_2)_6]$		
	: 0 11	(3 05 Å)	M: Na, K, Rb and Cs		
$f(Rb^+ \cdot O)$	. 0.12	(2 95 Å)			
	: 0.10	(3 15 Å)	See Table 10		
$f(Cs^+ \cdot O)$	· 0 10	(3 15 Å)			
	: 0 08	(3 30 Å)			
$f(K^{+}\cdot O)$	0 12	(3 01 Å)	$K_2M[Ni(NO_2)_6]$		
$f(Ca^{2+}\cdot\cdot O)$	: 0 15	(2 77 Å)	M. Ca and Ba		
$f(K^{+}\cdot\cdot O)$	: 0 10	(3 13 Å)	See Table 10		
$f(Ba^{2+} \cdot O)$	0 12	(2 93 Å)			
$f(K^{+}\cdot N)$	0 15	(2 5 Å~)			
	: 0 12	(3 0 Å~)	$K_3[Fe(CN)_6]$ and		
	: 0.01	(3.8 Å~)	$K_3[Cr(CN)_6]$		
$f(K\cdots{}^+C)$	: 0 04	(3 1 Å~)	See Table 16		
	. 0 02	(3.5 Å~)			
f(H Cl)	0 18	(2 66 Å)	$[Ni(NH_3)_6]Cl_2$	:	110
	: 0 15	(2 97 Å)			
$f(H\cdot\cdot Br)$	: 0 17	(2.77 Å)	$[Ni(NH_3)_6]Br_2$		90
	: 0.14	(3 07 Å)			
$f(H \cdot I)$	: 0 15	(2 97 Å)	$[Ni(NH_3)_6]I_2$	:	81
	: 0 12	(3 25 Å)			

* The second column gives the values of the potential constants in md/Å and the last column gives the infrared frequencies in cm^{-1} which contribute primarily to determine the potential constants

[a] refs. 22d, 22f, 32, [b] refs. 22e, 22f, 22h; [c] refs. 21, 25; [d] refs 22a, 28; [e] ref. 14, [f] ref. 14; [g] ref. 33; [h] ref. 5; [i] refs 24, 26, 28, 32

with the orthorhombic structure with the space group D_{2h}^{14} but can be explained only on the basis of the monoclinic structure as discussed above.

Bloor interpreted all the bands observed below 110 cm^{-1} for $K_3[Fe(CN)_6]$ as inner C–M–C deformation modes[31], on the basis of the argument that, for the orthorhombic structure, the inner C–M–C deformation modes of "g" species are observed in the infrared (see Table 15 (b)). However, the experimental results (temperature effect) in Fig. 14 and the results of the calculation in Table 16 for $K_3[Cr(CN)_6]$ and$Cs_3[Cr(C N)_6]$, can hardly support his interpretation.

E. SUMMARY VIEW

(1) *Potential constants*

The interionic potential constants of diatomic crystals were given (B, iii) using alkali halides as examples Then the potential constants which govern the so called ionic crystals, perovskite and rutile fluorides, were obtained on the basis of the molecular dynamical model, followed by the interionic potential constants between the complex ion and outer ion as well as the intramolecular force constants in the complex ion for some basic complex salts such as hexanitro- and hexacyano-complex salts. For the interionic potential in the complex salts, the interpretation was made on the basis of the molecular dynamical model that this term arises from the interaction between the outer ions and the neighbouring atoms of the complex ions.

The interactions are usually taken for atompairs whose distances are shorter than 4.0 Å. There are several other studies not mentioned in the present review, performed in a similar manner, the halogeno-complex salts by Hiraishi and Shimanouchi[32], the ammine complex salts by Nakagawa and Shimanouchi[26], the transition metal oxides by Nakagawa *et al.*[14], and some inorganic crystals such as CaF_2, ZnS, etc, by Tsuboi *et al*[4,33]. Table 18 summarizes the potential constants given in these studies, together with those obtained in the previous sections of the present review.

First it can be seen that the values of the force constants for the coordination bonds vary from 0.20 md/Å to 3.0 md/Å. Since the values of the force constants for the typical ionic bonds are about 0.1 md/Å, all of the force constants given in (b) and (c) reveal that these bonds include more or less covalent character. It should be noted that some amount of covalent character is included in the M–F bond of the so-called ionic crystal KMF_3. This is consistent with a theoretical study (SCF molecular orbital theory) by Sugano and Tanabe which showed some degree of covalent character[34] in the Ni–F bond of $KNiF_3$. However, comparing the values of the M–F stretching force constants with those of PtF_6 (a) and $[PtF_6]^{2-}$ (b1), it is concluded that the M–F bond in the perovskite fluoride is much weaker

and less covalent. In relation to this, it may be seen that the M–O bond in the transition metal oxide (NaCl-type crystal) is of the same order of covalent character as for the M–F bond in the above KMF_3, since both of the force constants amount to 0.60 ~ 0 80 md/Å [(b5) and (b6)]. It is interesting that both $KNiF_3$ and NiO exhibit antiferromagnetism below the Néel temperature, suggesting electron delocalization in the Ni–F and Ni–O bonds

Interaction potential constants which are the expression of the interaction between the complex ion and the outer ion and which mainly govern the lattice vibration frequencies, amount to 0.15 ~ 0 01 md/Å, depending upon the interatomic distances. It is clear that the interaction potential constants are closely related to the distances of the atompairs However, besides this the electrostatic factors such as the effective charges and polarizabilities of both atoms may be the other factors to determine the interaction potential constants, as Rittner proposed for the potential of alkali halide gases[35]. The interpretation for these interaction constants on a theoretical basis and the comparison of these values with those calculated from a non-empirical formula such as Rittner's equation, remain to be studied in the future. It should be noted that a normal coordinate analysis of the optically active vibrations of the crystal on the basis of the molecular dynamical model is useful for the interpretation of the lattice vibrations as well as the inner vibrations of the complex salts.

(ii) Vibrational coupling between the lattice modes and the intramolecular modes

It was known that the lattice vibrations are located below 200 cm^{-1} whereas the low-frequency inner vibrations in the complex ion such as skeletal deformation modes are also observed in the region 300 cm^{-1} to 100 cm^{-1}. Therefore, proper vibrational frequencies for both of these modes are quite often overlapped and these modes are coupled with each other in a complex manner. The vibrations for which the displacements of the outer ions relative to the complex ion are predominant and have frequencies which change markedly with the outer ions, may be qualified as lattice vibrations. However, the vibrational frequencies below 300 cm^{-1} vary more or less with the outer ions. For example, one can see how the lattice vibrations due to the interaction between the complex ion and the outer ion have an effect upon the inner vibration frequencies In Tables 10 and 16 for the hexanitro- and hexacyano-complex salts, there are frequency changes with the outer ion and also frequency differences between the calculated frequencies including the interaction potential constants and those neglecting them. In Table 16 of $K_3[Cr(CN)_6]$ and $Cs_3[Cr(CN)_6]$, the bands in the region 150 cm^{-1} to 100 cm^{-1} can be defined either as inner C–M–C deformation modes or as lattice modes.

In the more simple case of $K_2[PtCl_4]$, the displacement of each atom for the infrared active in-plane vibrations of the E_u species is drawn in Fig. 15, on

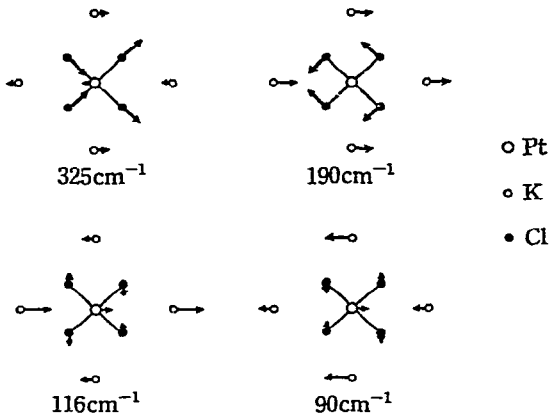

Fig. 15. Vibrational modes of E_u species vibrations of $K_2[PtCl_4]$

TABLE 19

OBSERVED AND CALCULATED FREQUENCIES (cm^{-1}) OF $K_2[PtCl_4]$

Species	*Spectrum*	*Obs*	*Calc I*[a]	*Calc II*[b]
a_{1g}	Raman	335	335	335
b_{1g}	Raman	164	164	164
b_{2g}	Raman	304	304	304
a_{2u}	IR	170	175	123
		103	100	0
e_u	IR	325	325	325
		190	192	142
		116	110	0
		90	87	0

[a] Calc I· including interaction constant f(K· Cl) = 0 115 md/Å
[b] Calc II. without interaction constant

the basis of the calculated result by Hiraishi and Shimanouchi[32]. The 190 cm^{-1} vibration is assigned to the Cl–Pt–Cl deformation mode with an appreciable component of the lattice mode whereas the vibrations at 116 cm^{-1} and 90 cm^{-1} are assigned to the translational lattice modes with a small component of the inner vibration. Table 19 lists the calculated frequencies with and without the interaction potential constant, from which one can see clearly the effect of the outer ions upon the inner vibrations.

As a summary of the outer ion effect upon the inner vibrations, considering the results in Tables 10, 17 and 19, it is concluded that the metal–ligand stretching vibration usually located in the region above 300 cm^{-1} is not affected by the outer ion effect. It may be said that the metal–ligand stretching frequency and the corresponding force constant, which is one of the important criteria for the metal–ligand interaction, may be reasonably interpreted on the basis of the isolated complex ion without considering the outer ions. The above conclusion is very

important from the physical point of view, since there are many complex salts whose crystal structures including the outer ions are not determined, however the study of the metal–ligand interaction in the complex ion through the vibrational spectrum is an important subject in coordination chemistry.

ACKNOWLEDGMENT

The author wishes to express his sincere thanks to Prof. T. Shimanouchi of University of Tokyo for his kind guidance and valuable discussions of the subjects described in this review. Thanks are also due to Rev. Father J. L. Walter, C S.C. of University of Notre Dame, for his generous reading and correction of the manuscript and useful discussions.

REFERENCES

1 See, for example, M Born and K Huang, *Dynamical Theory of Crystal Lattices*, Oxford Univ Press, 1966.
2 See, for example, S Bhagavantam and T. Venkatarayudu, *Theory of Groups and Its Applications to Physical Problems*, 2nd. ed , Andhra Univ., Waltair, 1951, p 127
3 E B Wilson, Jr , *J Chem. Phys* , 7 (1939) 1047; 9 (1941) 76
4 T. Shimanouchi, M Tsuboi and T. Miyazawa, *J Chem Phys* , 35 (1961) 1597
5 F. A Miller, in P. W Hepple, (Ed), *Far Infrared Spectroscopy*, London, 1969.
6 V. Barkhatov, *Acta Physicochim URSS*, 16 (1942) 123; see also, N A Curry and W A Runciman, *Acta Cryst* , 12 (1959) 674.
7 I Harada and T. Shimanouchi, *J Chem. Phys* , 46 (1967) 2708
8 See, for example, W. G Spitzer and D A Kleinman, *Phys Rev* , 121 (1961) 1324
9 G R Hunt, C H Perry and J. Ferguson, *Phys Rev* , 134 (1964) A688; C H Perry, *Japanese J Appl Phys* , 4 (1965), *Suppl I*, 564
10 M. Balkanski, P Moch and G. Parisot, *J Chem. Phys* , 44 (1966) 940.
11 A S Barker, Jr , *Phys. Rev* , 136 (1964) A1290
12 R W. G. Wyckoff, *Crystal Structures*, Interscience Publishers, Inc , New York, 1948, Vol 2, Chap 7.
13 A Tsuchida, *J. Phys. Soc. Japan*, 21 (1966) 2497, A Tsuchida and I. Nakagawa, *ibid* , 20 (1965) 1726.
14 I Nakagawa, A Tsuchida and T. Shimanouchi, *J. Chem Phys* , 47 (1967) 982.
15 W. Rudorff, J. Kandler and D. Babel, *Z, Anorg Allgem. Chem* , 317 (1962) 261
16 A F Wells, *Structural Inorganic Chemistry*, 3rd Ed , Oxford Univ Press, 1962, p 497
17 T Shimanouchi, I Nakagawa, J. Hiraishi and M Ishii, *J Mol Spectry* , 19 (1966) 78
18 R. W. G. Wyckoff, *Crystal Structures*, Interscience Publishers, Inc , New York, 1951, Vol 1, Chap 4; J. W. Stout and S A Reed, *J Amer. Chem Soc* , 76 (1954) 5279.
19 S P. S. Porto, P. A Fleury and T. C. Damen, *Phys Rev* , 154 (1967) 522
20 R. W. G Wyckoff, *Crystal Structures*, Interscience Publishers, Inc , New York, 1951, Vol 2, Chapters 9 and 10, M. Driel and H J Verweell, *Z Krist* , A95 (1936) 308
21 I Nakagawa, T. Shimanouchi and K Yamasaki, *Inorg Chem* , 7 (1968) 1332
22 (a) T Shimanouchi and I Nakagawa, *Spectrochim Acta*, 18 (1962) 89, (b) I Nakagawa and T. Shimanouchi, *ibid* , 18 (1962) 101; (c) I Nakagawa and T. Shimanouchi, *ibid* , 20 (1964) 429, (d) J. Hiraishi, I. Nakagawa and T Shimanouchi, *ibid* , 20 (1964) 819; (e) T. Shimanouchi and I Nakagawa, *Inorg Chem* , 3 (1964) 1805; (f) I Nakagawa and

T. SHIMANOUCHI, *Spectrochim Acta*, 22 (1966) 759; (g) M. MIKAMI, I NAKAGAWA AND T SHIMANOUCHI, *ibid*, 23A (1967) 1037; (h) J. HIRAISHI, I. NAKAGAWA AND T. SHIMANOUCHI, *ibid.*, 24A (1968) 819

23 I. NAKAGAWA, *Proceedings 10th International Conference on Coordination Chemistry, Nikko, Japan, Sept. 1967.*

24 I NAKAGAWA, T. SHIMANOUCHI AND K. YAMASAKI, *Inorg Chem*, 3 (1964) 772.

25 I. NAKAGAWA AND T SHIMANOUCHI, *Spectrochim Acta*, 23A (1967) 2099.

26 I NAKAGAWA AND T. SHIMANOUCHI, *ibid*, 22 (1966) 1707.

27 L SACCONI, A. SABATINI AND P. GANS, *Inorg Chem*, 3 (1964) 1772

28 I NAKAGAWA AND T SHIMANOUCHI, *Spectrochim. Acta*, 25A (1969)

29 L. H JONES, *Inorg. Chem*, 2 (1963) 777.

30 J A. KOHN AND W. D. TOWNES, *Acta Cryst*, 14 (1961) 617.

31 D. BLOOR, *J. Chem. Phys.*, 41 (1964) 2573.

32 J. HIRAISHI AND T. SHIMANOUCHI, *Spectrochim Acta*, 22 (1966) 1483.

33 M. TSUBOI, *J Chem. Phys.*, 40 (1964) 1326, M. TSUBOI AND A WADA, *ibid*, 48 (1968) 2615.

34 S SUGANO AND Y TANABE, *J Phys Soc. Japan*, 20 (1960) 1155.

35 E. S RITTNER, *J. Chem. Phys.*, 19 (1951) 1030